Check for updates

American Society of Hematology
2021 L Street NW, Suite 900,
Washington, DC 20036
Phone: 202-776-0544 | Fax 202-776-0545
editorial@hematology.org

Gasdermin D drives focal Crystalline Thrombotic Microangiopathy by accelerating Immunothrombosis and Necroinflammation

Tracking no: BLD-2023-021949R3

Kanako Watanabe-Kusunoki (Department of Rheumatology, Endocrinology and Nephrology, Faculty of Medicine and Graduate School of Medicine, Hokkaido University, Sapporo, Japan, Japan) Chenyu Li (LMU Hospital, Germany) Tâmisa Seeko Bandeira Honda (Renal Division, Department of Medicine IV, LMU University Hospital, LMU Munich, Germany, Germany) Danyang Zhao (Renal Division, Department of Medicine IV, LMU University Hospital, LMU Munich, Germany, Germany) Yoshihiro Kusunoki (Department of Rheumatology, Endocrinology and Nephrology, Faculty of Medicine and Graduate School of Medicine, Hokkaido University, Sapporo, Japan, Japan) John Ku (Renal Division, Department of Medicine IV, LMU University Hospital, LMU Munich, Germany, Germany) Hao Long (, China) Martin Klaus (Renal Division, Department of Medicine IV, LMU University Hospital, LMU Munich, Germany, Germany) Chao Han (Renal Division, Department of Medicine IV, LMU University Hospital, LMU Munich, Germany, Germany) Attila Braun (Walther Straub Institute, LMU, Muenchen, Germany) Elmina Mammadova-Bach (Walther-Straub-Institute for Pharmacology and Toxicology, Ludwig-Maximilians-University, Munich, Germany, Germany) Andreas Linkermann (Department of Internal Medicine 3, University Hospital Carl Gustav Carus at the Technische Universität Dresden, Dresden, Germany, Germany) Kristof Avondt (Institute of Experimental Pathology (ExPat), Centre of Molecular Biology of Inflammation (ZMBE), University of Münster, Münster, Germany, Germany) Mathis Richter (Institute of Experimental Pathology (ExPat), Centre of Molecular Biology of Inflammation (ZMBE), University of Münster, Münster, Germany, Germany) Oliver Soehnlein (Institute of Experimental Pathology (ExPat), Centre of Molecular Biology of Inflammation (ZMBE), University of Münster, Münster, Germany, Germany) Monika Linder (Ludwig-Maximilians-Universität München, Germany) Christoph Klein (LMU Klinikum, Dr. von Hauner Childrens Hospital, LMU Klinikum, Germany) Stefanie Steiger (LMU Hospital, Germany) Hans-Joachim Anders (Poliklink, LMU, Germany)

Abstract:
Thrombotic microangiopathy (TMA) is characterized by immunothrombosis and life-threatening organ failure, but the precise underlying mechanism driving its pathogenesis remains elusive. In this study, we hypothesized that gasdermin D (GSDMD), a pore-forming protein serving as the final downstream effector of pyroptosis/interleukin (IL)-1□□pathway, contributes to TMA and its consequences by amplifying neutrophil maturation and subsequent necrosis. Using a murine model of focal crystalline TMA, we found that Gsdmd-deficiency ameliorated immunothrombosis, acute tissue injury and failure. Gsdmd-/- mice exhibited a decrease in mature IL-1□, as well as in neutrophil maturation, □2 integrin activation, and recruitment to TMA lesions, where they formed reduced neutrophil extracellular traps both in arteries and interstitial tissue. The GSDMD inhibitor disulfiram dose-dependently suppressed human neutrophil pyroptosis in response to cholesterol crystals. Experiments with GSDMD-deficient human induced pluripotent stem cell-derived neutrophils confirmed the involvement of GSDMD in neutrophil □2 integrin activation, maturation as well as pyroptosis. Both prophylactic and therapeutic administration of disulfiram protected mice from focal TMA, acute tissue injury and failure. Our data identify GSDMD as a key mediator of focal crystalline TMA and its consequences: ischemic tissue infarction and organ failure. GSDMD could potentially serve as a therapeutic target for systemic forms of TMA.

Conflict of interest: No COI declared

COI notes:

Preprint server: No;

Downloaded from http://ashpublications.net/blood/article-pdf/doi/10.1182/blood.2023021949/2223568/blood.2023021949.pdf by guest on 06 May 2024

Author contributions and disclosures: H-J.A and S.S.: Funding and supervision. K.W-K., S.S., and H-J.A.: Conceptualization. K.W-K. and S.S.: Methodology. K.W-K.: Investigation. K.W-K., C.L., K.J., L.H., H.C., and M.K.: Data analysis. K.W-K., E.M-B., K.V.A., M.R., and O.S.: Visualization. M.I.L. and C.K.: Differentiation of iPSC-derived neutrophils with gene editing. K.W-K., H.C., B.A., and E.M-B.: Flow chamber experiments. T.S.B.H., D.Z., and Y.K.: Protocol and suggestions. A.L.: Resources. K.W-K. and H-J.A.: Writing original drafts. All authors read and revised the manuscript.

Non-author contributions and disclosures: No;

Agreement to Share Publication-Related Data and Data Sharing Statement: Data are available upon reasonable request to the corresponding author.

Clinical trial registration information (if any):

Downloaded from http://ashpublications.net/blood/article-pdf/doi/10.1182/blood.2023021949/2223568/blood.2023021949.pdf by guest on 06 May 2024

Gasdermin D drives focal Crystalline Thrombotic Microangiopathy by accelerating Immunothrombosis and Necroinflammation

Kanako Watanabe-Kusunoki[1,2], Chenyu Li[1], Tâmisa Seeko Bandeira Honda[1], Danyang Zhao[1], Yoshihiro Kusunoki[1,2], John Ku[1], Hao Long[1,3], Martin Klaus[1], Chao Han[1,4], Attila Braun[1,4], Elmina Mammadova-Bach[1,4], Andreas Linkermann[5,6], Kristof Van Avondt[7], Mathis Richter[7], Oliver Soehnlein[7], Monika I. Linder[8], Christoph Klein[8], Stefanie Steiger[1,#], Hans-Joachim Anders[1,#]

1 Renal Division, Department of Medicine IV, LMU University Hospital, LMU Munich, Germany
2 Department of Rheumatology, Endocrinology and Nephrology, Faculty of Medicine and Graduate School of Medicine, Hokkaido University, Sapporo, Japan
3 Department of Urology, The Affiliated Hospital of Southwest Medical University, Luzhou, China
4 Walther-Straub-Institute for Pharmacology and Toxicology, Ludwig-Maximilians-University, Munich, Germany
5 Department of Internal Medicine 3, University Hospital Carl Gustav Carus at the Technische Universität Dresden, Dresden, Germany
6 Division of Nephrology, Department of Medicine, Albert Einstein College of Medicine, Bronx, New York, United States
7 Institute of Experimental Pathology (ExPat), Centre of Molecular Biology of Inflammation (ZMBE), University of Münster, Münster, Germany
8 Department of Pediatrics, Dr. von Hauner Children's Hospital, University Hospital, Ludwig-Maximilians-Universität (LMU), Munich, Germany
# contributed equally.

Correspondence author
Hans-Joachim Anders, MD
Medizinische Klinik und Poliklinik IV, LMU Klinikum
Ziemssenstr. 5 80336 München, Germany
Phone: +49 89 4400 32623
Email: hjanders@med.uni-muenchen.de

Data are available upon reasonable request to the corresponding author.

Downloaded from http://ashpublications.net/blood/article-pdf/doi/10.1182/blood.2023021949/2223568/blood.2023021949.pdf by guest on 06 May 2024

37 **Running title:** Gasdermin D in TMA

38 Text word count: 4084, Abstract word count: 198, Figures: 7, Tables: 0, References: 39

Downloaded from http://ashpublications.net/blood/article-pdf/doi/10.1182/blood.2023021949/2223568/blood.2023021949.pdf by guest on 06 May 2024

Key Points

・Gasdermin D contributes to focal crystalline thrombotic angiopathy and its consequences: ischemic tissue infarction and organ failure.

・Gasdermin D drives neutrophil necrosis, maturation, and tissue recruitment during focal crystalline thrombotic angiopathy.

Downloaded from http://ashpublications.net/blood/article-pdf/doi/10.1182/blood.2023021949/2223568/blood.2023021949.pdf by guest on 06 May 2024

Abstract

Thrombotic microangiopathy (TMA) is characterized by immunothrombosis and life-threatening organ failure, but the precise underlying mechanism driving its pathogenesis remains elusive. In this study, we hypothesized that gasdermin D (GSDMD), a pore-forming protein serving as the final downstream effector of pyroptosis/interleukin (IL)-1β pathway, contributes to TMA and its consequences by amplifying neutrophil maturation and subsequent necrosis. Using a murine model of focal crystalline TMA, we found that *Gsdmd*-deficiency ameliorated immunothrombosis, acute tissue injury and failure. *Gsdmd*$^{-/-}$ mice exhibited a decrease in mature IL-1β, as well as in neutrophil maturation, β_2 integrin activation, and recruitment to TMA lesions, where they formed reduced neutrophil extracellular traps both in arteries and interstitial tissue. The GSDMD inhibitor disulfiram dose-dependently suppressed human neutrophil pyroptosis in response to cholesterol crystals. Experiments with *GSDMD*-deficient human induced pluripotent stem cell-derived neutrophils confirmed the involvement of GSDMD in neutrophil β_2 integrin activation, maturation as well as pyroptosis. Both prophylactic and therapeutic administration of disulfiram protected mice from focal TMA, acute tissue injury and failure. Our data identify GSDMD as a key mediator of focal crystalline TMA and its consequences: ischemic tissue infarction and organ failure. GSDMD could potentially serve as a therapeutic target for systemic forms of TMA.

Keywords: Neutrophils, platelets, inflammation, innate immunity, neutrophil extracellular traps

Downloaded from http://ashpublications.net/blood/article-pdf/doi/10.1182/blood.2023021949/2223568/blood.2023021949.pdf by guest on 06 May 2024

Introduction

Thrombotic microangiopathy (TMA) is a heterogeneous group of diseases characterized by microvascular immunothrombosis and ischemic tissue injury, leading to organ failure. TMA may manifest in otherwise healthy individuals following exposure to bacterial toxins, i.e., Shiga toxin-associated hemolytic uremic syndrome. Furthermore, systemic TMA can arise either due to a deficiency in von Willebrand factor-cleaving protease (i.e., thrombotic thrombocytopenic purpura), or owing to dysregulation of the alternative complement pathway (i.e., atypical hemolytic uremic syndrome). These pathogenic conditions may be clinically expressed in either a hereditary or acquired manner following incidental triggers such as infections, certain drugs, pregnancy, or transplantation.[1,2] We recently described that injection of cholesterol crystals into the kidney artery of mice induces focal TMA, particularly involving renal thrombotic arterial occlusions, and subsequent ischemic kidney infarction and failure.[3] While focal TMA may not manifest typical signs of systemic TMA such as hemolytic anemia,[4] the key elements of microvascular immunothrombosis are similar.

Gasdermin D (GSDMD) is a pore-forming protein.[5] Upon activation, GSDMD translocates from the cytosol into the plasma membrane via its N-terminal domain, where it forms pores. GSDMD pores facilitate the secretion of mature interleukin (IL)-1β and IL-18 but also promote membrane rupture, i.e., pyroptosis, a highly inflammatory form of regulated necrosis in myeloid cells downstream of inflammasome activation.[6,7] In addition, GSDMD has been implicated in the release of neutrophil extracellular traps (NETs).[8-10] In neutrophils, neutrophil elastase can activate GSDMD in an inflammasome-independent manner, which in turn promotes further release and activation of neutrophil elastase, histone cleavage, and chromatin decondensation, an early stage of NET

Downloaded from http://ashpublications.net/blood/article-pdf/doi/10.1182/blood.2023021949/2223568/blood.2023021949.pdf by guest on 06 May 2024

formation.[8] While these proinflammatory cell death mechanisms contribute to host defense against pathogens, their dysregulation can cause unnecessary tissue damage also in sterile diseases.[11]

Circulating particles can activate the nucleotide oligomerization domain-like receptor protein 3 (NLRP3) inflammasome,[12,13] and induce neutrophils to release NETs.[14] NETs also elicit a potent procoagulant response by recruiting and activating platelets.[15] These processes can accelerate necroinflammation and immunothrombosis. Therefore, we hypothesized that GSDMD contributes to focal crystalline TMA by amplifying neutrophil necrosis; thus facilitating immunothrombosis within the vasculature and enhancing subsequent necroinflammation of ischemic tissue.

Materials and Methods

A detailed description of the Materials and Methods is provided in the online Supplement file.

Animal experiments

C57BL/6N mice were obtained from Charles River Laboratories (Sulzfeld, Germany). The *Gsdmd*$^{-/-}$ mice were provided by Prof. Andreas Linkermann from the Technische Universität Dresden. All mice were housed in groups of five under Specific Pathogen-Free conditions with enrichment and had access to food and water. All experimental procedures were approved by the local government authorities Regierung von Oberbayern (reference number: ROB-55.2-2532.Vet_02-19-79) based on the European Union directive for the Protection of Animals Used for Scientific Purposes (2010/63/EU) and reported according to the Animal Research: Reporting of In Vivo Experiments

Downloaded from http://ashpublications.net/blood/article-pdf/doi/10.1182/blood.2023021949/2223568/blood.2023021949.pdf by guest on 06 May 2024

guidelines.[16]

Isolation of human blood neutrophils

Human blood neutrophils were isolated from healthy individuals using dextran sedimentation, followed by Ficoll-Hypaque density centrifugation procedures as previously described.[17,18] The cells were suspended in Hanks' Balanced Salt Solution (HBSS) supplemented with 2% fetal calf serum. The study to obtain whole blood samples from healthy individuals received approval from the local Ethical Review Board of the Medical Faculty at the LMU Munich (reference number: 21-0522), and written informed consent was acquired from all participants.

Maintenance and differentiation of human induced pluripotent stem (iPS) cells

iPS cells were maintained on a tissue culture dish coated with growth factor-reduced Matrigel (#356231, Corning) in mTeSR1 serum-free medium (#5850, Stemcell). Differentiation towards neutrophil-like granulocytes was initiated as outlined in the online Supplement file.

Statistical analysis

Statistical analysis was performed using GraphPad Prism 7 software (GraphPad, La Jolla, CA, USA). For in vivo data, the mean ± SD is presented, and the Student's t-test was utilized to determine the significance between two groups. For comparing three or more groups, one-way analysis of variance (ANOVA) with Tukey's post-hoc test was used. When two parameters with multiple groups were employed, two-way ANOVA with Bonferroni's multiple comparisons test was performed. For in vitro data, the mean ± SEM

Downloaded from http://ashpublications.net/blood/article-pdf/doi/10.1182/blood.2023021949/2223568/blood.2023021949.pdf by guest on 06 May 2024

is presented, and one-way ANOVA with Dunnett's multiple comparisons test was carried out to compare three or more groups. When two or more parameters with multiple groups were used, two-way ANOVA with Dunnett's multiple comparisons test was performed. Statistical significance was determined by P values of less than 0.05, which were indicated as *$p < 0.05$, **$p < 0.01$, and ***$p < 0.001$.

All animal experimental procedures were approved by the local government authorities Regierung von Oberbayern based on the European Union directive for the Protection of Animals Used for Scientific Purposes. The study to obtain whole blood samples from healthy individuals received approval from the local Ethical Review Board of the Medical Faculty at LMU Munich, and written informed consent was acquired from all participants.

Results

GSDMD is expressed in neutrophils during their maturation and is activated upon focal crystalline TMA

To investigate the expression and activation of GSDMD in neutrophils during ischemic inflammation, we conducted single-cell RNA sequencing analysis using a previously published dataset.[19] The dataset was based on cells sorted from kidney, blood, and spleen of C57BL/6J mice before and after unilateral kidney ischemia-reperfusion injury (Figure 1A) and contained a total of 80,829 cells, which were grouped in 26 clusters after quality control (Figure 1B). Clusters 3 and 15 were identified as neutrophils based on the expression of specific transcripts (Supplementary figure S1A). Further categorization of these neutrophils into eight clusters (G0-4 and G5a-c) based on their differentiation stages[20] (Supplementary table S1) revealed that clusters G0, G1, G2, and G3 correspond to granulocyte-monocyte progenitor, pro-neutrophil, pre-neutrophil, and immature

Downloaded from http://ashpublications.net/blood/article-pdf/doi/10.1182/blood.2023021949/2223568/blood.2023021949.pdf by guest on 06 May 2024

neutrophil, respectively, and primarily derived from spleen and blood (Figures 1C, Supplementary figures S1B-S1D). Conversely, clusters G4 and G5a-c represent mature neutrophils from the spleen, blood, and kidney post-injury, respectively. *Gsdmd* transcripts were mainly detected in immature and mature neutrophils in all organs (Figures 1D and 1E). Thus, neutrophil maturation involves the constitutive expression of Gsdmd and Gsdmd-positive mature neutrophils migrate to the injured kidney.

Next, to elucidate the involvement of neutrophils in cholesterol crystal (CC)-induced TMA, we performed MACSima imaging using markers for neutrophils as well as cell death within the whole TMA kidneys and the contralateral sham kidneys from wild-type (WT) mice (Figure 1F). In the TMA kidney, smooth muscle actin (SMA)-positive arteries showed the presence of CD41-positive platelets within thrombi (further supported by Figure 1G), together with neutrophils which formed NETs manifested by colocalization of Ly6G and citrullinated histone 3 (CitH3). A significant accumulation of neutrophils was noted in the periinfarct region. Moreover, the kidney cortex revealed widespread parenchymal cell death, as indicated by the presence of cleaved caspase-3-positive cells. These findings suggest that neutrophils actively participate to both TMA lesions as well as ischemic tissue infarction.

Furthermore, we investigated whether Gsdmd is expressed and activated in TMA kidneys. Immunohistochemistry revealed Gsdmd positivity in peritubular interstitial cells of TMA kidneys from WT mice as compared to sham kidneys (Figure 1H). In contrast, no signal was detected in TMA kidneys from *Gsdmd*$^{-/-}$ mice, demonstrating specificity of the Gsdmd antibody. Immunoblot analysis performed on total kidneys further demonstrated increased expression of the cleaved N-terminal fragment of Gsdmd and cleaved caspase-1 in TMA kidneys from WT mice as compared to kidneys from healthy

Downloaded from http://ashpublications.net/blood/article-pdf/doi/10.1182/blood.2023021949/2223568/blood.2023021949.pdf by guest on 06 May 2024

controls (Figure 1I). Importantly, immunoblot analysis performed on immune cells isolated from WT TMA kidneys showed an increased expression of cleaved GSDMD (Figure 1J). Concurrently, flow cytometric analysis identified increased levels of activated caspase1-positive neutrophils in WT TMA kidneys (Figures 1K and 1L). These findings suggest Gsdmd activation in the crystalline TMA kidney and substantiate its association with infiltrating immune cells including neutrophils.

Gsdmd deficiency attenuates focal TMA and its consequences

To investigate the role of GSDMD in focal TMA, we used *Gsdmd*$^{-/-}$ mice and WT mice (Supplementary figure S2A). TMA was induced by injecting CC (20 mg/kg) into the left kidney artery, and the mice were sacrificed 24 hours post-induction (Figure 2A). *Gsdmd*-deficiency reduced the number of arteries and glomerular microvessels obstructed by crystal clots (Figures 2B-2F). In comparison to WT mice, *Gsdmd*$^{-/-}$ mice were partially protected from the sudden drop in glomerular filtration rate (GFR), i.e., acute kidney injury (AKI) (Figure 2G). Kidney infarct size was consistently reduced (Figures 2H and 2I) as was the tubular injury score (Figures 2J and 2K) and TdT-mediated dUTP-biotin nick end labeling (TUNEL) positivity of kidney cells (Supplementary figures S2B and S2C). Furthermore, *Gsdmd*-deficiency reduced the levels of mature IL-1β in the kidneys (Figure 2L), as well as the levels of circulating IL-1β and histone (Figure 2M, Supplementary figure S2D) following TMA. These data indicate that GSDMD contributes to focal crystalline TMA and its consequences, i.e., tissue infarction and organ failure.

Neutrophil recruitment and maturation are impaired in _Gsdmd_$^{-/-}$ mice with focal

Downloaded from http://ashpublications.net/blood/article-pdf/doi/10.1182/blood.2023021949/2223568/blood.2023021949.pdf by guest on 06 May 2024

TMA

To investigate the mechanisms underlying the improvement of the TMA phenotype in *Gsdmd*$^{-/-}$ mice, we focused on neutrophils, which are the first leukocytes recruited to inflammatory sites[21] (Figure 1F) and exhibit GSDMD expression during their maturation and sterile kidney inflammation (Figures 1D and 1E). Consequently, we examined the abundance of circulating and kidney-infiltrating neutrophils by flow cytometry (Figure 3A, Supplementary figures S3A and S3B). In contrast to WT mice, *Gsdmd*$^{-/-}$ mice after focal TMA showed reduced percentages and absolute numbers of neutrophils, recognized as CD45+ CD11b+ Ly6G+ cells in both blood (Figures 3B and 3C) and kidney (Figures 3D and 3E). Consistent with the flow cytometric analysis, immunohistochemistry displayed reduced amounts of Ly6G-positive neutrophils infiltrating the TMA kidney in *Gsdmd*$^{-/-}$ mice compared to WT mice (Supplementary figures S3G and S3H). In contrast, the numbers of monocytes (CD45+ CD11b+ Ly6C+) in kidney and blood were unaffected (Supplementary figures S3C-S3F).

To comprehend the difference in neutrophil recruitment from bone marrow to blood and kidney, we analyzed the percentages and absolute numbers of neutrophils in bone marrow, spleen, and lung (Supplementary figures S4A-S4C). However, neither neutrophil numbers nor monocyte numbers showed any significant differences (Supplementary figures S4D-S4O). Nevertheless, we examined neutrophil maturation in circulation and hematopoietic organs (Figure 3F). Interestingly, *Gsdmd*-deficiency reduced the fraction of mature neutrophils identified as CD45+ CD11b+ Ly6G+ CD101+ cells in bone marrow, spleen, and blood compared to WT mice following focal TMA (Figures 3G-3I). Correspondingly, the number of mature neutrophils in each organ was significantly decreased in *Gsdmd*$^{-/-}$ mice following focal TMA (Figures 3J-3L). Baseline levels of

Downloaded from http://ashpublications.net/blood/article-pdf/doi/10.1182/blood.2023021949/2223568/blood.2023021949.pdf by guest on 06 May 2024

234 neutrophils and monocytes (Supplementary figures S5A-S5C), as well as the fraction of
235 mature neutrophils (Supplementary figures S5D and S5E) were comparable in both
236 groups under normal conditions. Additional in vitro experiments revealed that *Gsdmd*$^{-/-}$
237 bone marrow mature neutrophils showed reduced expression of CXCR2 in the presence
238 of the differentiation factor granulocyte colony-stimulating factor (G-CSF) or tumor
239 necrosis factor alpha (TNFα) after 24 hours in culture (Figure 3M), which is crucial for
240 the neutrophil egress from bone marrow to blood.[22]

241 Furthermore, we performed flow cytometric analysis to look at β_2 integrin
242 macrophage-1 antigen (MAC-1) expression, which plays a crucial role in facilitating
243 neutrophil migration into inflamed tissues,[23,24] on bone marrow neutrophils. We observed
244 an increased expression of MAC-1 in bone marrow neutrophils from WT mice following
245 focal TMA compared to healthy WT mice, while MAC-1 expression was diminished
246 significantly in *Gsdmd*$^{-/-}$ mice with focal TMA (Figure 3N). These findings indicate that
247 neutrophil maturation as well as β_2 integrin activation are impaired in *Gsdmd*$^{-/-}$ mice with
248 focal TMA, leading to reduced neutrophil migration from bone marrow to blood and
249 kidneys, thus contributing to the attenuated TMA phenotype.

250

251 **_Gsdmd_ deficiency reduces NETs in both kidney arteries and tissue**
252 **necroinflammation in focal TMA**

253 The release of NETs from neutrophils can contribute to immunothrombosis and
254 necroinflammation, hence we performed immunofluorescence staining for markers of
255 NETs. *Gsdmd* deficiency reduced the formation of intravascular NETs in the kidneys,
256 identified as CitH3-positive area originating from Ly6G-positive neutrophils within
257 αSMA-positive arteries (Figures 4A and 4C). Additionally, *Gsdmd* deficiency led to a

Downloaded from http://ashpublications.net/blood/article-pdf/doi/10.1182/blood.2023021949/2223568/blood.2023021949.pdf by guest on 06 May 2024

decrease in intravascular occlusion involving neutrophils, platelets, and the area containing both neutrophils and platelets (Figures 4B and 4D-4F). Furthermore, *Gsdmd* deficiency reduced NET formation in kidney interstitial tissue (Figures 4G and 4H). This observation was further supported by a decrease in the absolute number of NETing neutrophils in the kidneys, undergoing cell death identified by flow cytometry as Ly6G and CitH3 double-positive cells (Figure 4I, Supplementary figure S6). These data indicate that GSDMD plays a crucial role in neutrophil- and NET-mediated immunothrombosis and necroinflammation in TMA.

Disulfiram inhibits CC-induced neutrophil pyroptosis in human neutrophils

We postulated that neutrophils could potentially function as cellular source of GSDMD in TMA. This is supported by the observation that neutrophils predominantly infiltrated the kidney within 24 hours following crystal injection (Figure 3D), the presence of activated GSDMD and caspase1 in immune cells including neutrophils within TMA kidneys, (Figures 1J-1L), and by our finding that the absence of *Gsdmd* in tubular epithelial cells did not impact on the levels of hypoxia-induced necrosis (Supplementary figure S7). Next, we examined the role of GSDMD in CC-induced neutrophil activation and death *in vitro*. Human neutrophils, primed with lipopolysaccharide (LPS) and exposed to increasing doses of CC, dose-dependently released IL-1β (Figure 5A). Immunoblot analysis showed that LPS/CC stimulation induced GSDMD cleavage, resulting in a subsequent increase of mature IL-1β in the supernatant (Figure 5B). Disulfiram (DSF), an inhibitor of GSDMD pore formation without affecting other inflammasome components,[6,25] dose-dependently reduced this effect, while receptor-interacting protein kinase 1 and mixed lineage kinase domain-like inhibitors, and a

Downloaded from http://ashpublications.net/blood/article-pdf/doi/10.1182/blood.2023021949/2223568/blood.2023021949.pdf by guest on 06 May 2024

caspase-1 inhibitor had no effect on IL-1β release (Figure 5C). These results suggest that GSDMD, rather than neutrophil necroptosis, is involved in IL-1β release. The same was noted for lactate dehydrogenase (LDH) release, a marker of cell necrosis, indicating that CC triggers GSDMD-dependent neutrophil pyroptosis rather than necroptosis (Figure 5D). Of note, the IL-1 receptor antagonist anakinra did not affect IL-1β release and GSDMD cleavage in CC-stimulated neutrophils (Supplementary figure S8), suggesting that the IL-1β pathway does not reciprocally influence GSDMD cleavage and the subsequent release of IL-1β.

Experiments using SYTOX Green (SG), a marker of cell death, showed increased SG signal in CXCL8-primed human neutrophils in a CC dose-dependent manner (Supplementary figure S9A). Furthermore, fluorescence microscopy confirmed that CC exposure promoted NET formation, characterized by web-like structures of extracellular DNA decorated with granule proteins (Figure 5E). However, despite DSF treatment on CC-stimulated neutrophils, NET formation was still observed (Figure 5E) and SG positivity was not reduced, unlike the effects seen with diphenyleneiodonium chloride, an inhibitor of nicotinamide adenine dinucleotide phosphate oxidase, which served as a control for CC-induced NET inhibition (Figures 5F and 5G). Thus, these findings indicate that GSDMD contributes to CC-induced neutrophil pyroptosis but not CC-induced NETosis.

Notably, histone, a known soluble NETs inducer,[17] showed reduced NETs induction as indicated by decreased levels of SG positivity in DSF-treated human neutrophils (Supplementary figures S9B-S9D). Histone stimulation did not induce IL-1β release in neutrophils (Supplementary figure S9E). Consistently, bone marrow neutrophils derived from *Gsdmd*$^{-/-}$ mice showed comparable levels of CC-induced NET formation but

Downloaded from http://ashpublications.net/blood/article-pdf/doi/10.1182/blood.2023021949/2223568/blood.2023021949.pdf by guest on 06 May 2024

306 diminished histone-induced NET formation in contrast to those from WT mice
307 (Supplementary figure S10). Furthermore, *Gsdmd*-deficiency prevented neutrophil
308 adhesion and NET formation on the CC-activated platelet-induced thrombi (Figures 5H-
309 5K, Supplementary figure S11). Together, these findings suggest that GSDMD modulates
310 not CC-induced but histone-induced NETosis, as well as NETosis triggered by CC-
311 activated platelets.
312
313 ***GSDMD*-deficient iPSC-derived human neutrophils resist CC-induced pyroptosis**
314 **and β_2 integrin activation**
315 To validate the findings observed with pharmacological inhibitors, we used a genetic
316 approach and generated *GSDMD*-deficient human iPSC-derived neutrophils by CRISPR-
317 Cas9-mediated gene editing. The absence of GSDMD in iPSC-derived neutrophils was
318 confirmed through immunoblot and Sanger sequencing of two distinct clones (Figure 6A,
319 Supplementary figure S12A). Notably, GSDMD protein expression increased in
320 differentiated control iPSC-derived neutrophils towards mature neutrophils (Figure 6B).
321 The number of live floating neutrophils and their maturation states were comparable
322 between the control and *GSDMD*-knockout clones (Supplementary figures S12B and
323 S12C). Fluorescence microscopy revealed cytoplasmic expression of GSDMD
324 colocalizing with myeloperoxidase (MPO) in control iPSC-derived neutrophils
325 (Supplementary figure S12D). *GSDMD*-knockout clones primed with LPS and exposed
326 to CC showed reduced levels of IL-1β and LDH in the cell culture supernatants compared
327 to the control iPSC-derived neutrophils (Figures 6C and 6D, Supplementary figure S13).
328 Furthermore, flow cytometric analysis demonstrated reduced activation of β_2 integrins,
329 lymphocyte function associated antigen 1 (LFA-1), and MAC-1 in *GSDMD*-knockout

Downloaded from http://ashpublications.net/blood/article-pdf/doi/10.1182/blood.2023021949/2223568/blood.2023021949.pdf by guest on 06 May 2024

clones (Figures 6E and 6F). *GSDMD*-knockout clones formed NETs upon CC stimulation similar to control iPSC-derived neutrophils (Figure 6G) and did not show a decrease in the inducibility quantified by SG positivity (Figures 6H and 6I). Collectively, these data confirm the involvement of GSDMD in CC-induced neutrophil pyroptosis, rather than NETosis, and β_2 integrin activation.

Disulfiram protects mice from TMA, AKI and ischemic infarction

To investigate the therapeutic potential of targeting GSDMD, we administered DSF to WT mice either 4 hours prior (prophylactic) or 3 hours following (therapeutic) CC injection, and assessed AKI and ischemic infarction (Figure 7A, Supplementary figure S14A). Compared to vehicle-treated controls, both prophylactic and therapeutic DSF treatment reduced the number of arteries affected by focal crystalline TMA (Figures 7B and 7C, Supplementary figures S14B and S14C). Both treatment regimes protected mice from the sudden drop of GFR, preventing AKI (Figure 7D, Supplementary figure S14D). Consistently, both prophylactic and therapeutic DSF treatments reduced ischemic infarction (Figures 7E and 7F, Supplementary figures S14E and S14F) and tubular injury scores (Figures 7G and 7H, Supplementary figures S14G and S14H). Flow cytometric analysis demonstrated a reduction in the absolute numbers of blood neutrophils and monocytes in both treatment groups (Figures 7I-7K, Supplementary figures S14I-S14K and S15), as well as a decrease in the percentages and absolute numbers of kidney-infiltrating neutrophils (Figures 7L and 7M, Supplementary figures S14L and S14M). Moreover, both treatments reduced NET formation in the TMA kidney (Figure 7N, Supplementary figure S14N). Taken together, both prophylactic and therapeutic DSF

Downloaded from http://ashpublications.net/blood/article-pdf/doi/10.1182/blood.2023021949/2223568/blood.2023021949.pdf by guest on 06 May 2024

353 treatments improved focal TMA-induced AKI and kidney infarction by ameliorating clot
354 formation as well as neutrophil-mediated necroinflammation.
355
356 **Discussion**
357 We had hypothesized that GSDMD plays a role in the pathogenesis of (crystalline)
358 TMA by promoting intravascular immunothrombosis and its subsequent outcomes,
359 including ischemic necroinflammation and organ failure. Our experiments revealed that
360 *Gsdmd*-deficiency alleviated CC-induced focal TMA, AKI, and ischemic kidney
361 infarction. We observed that GSDMD contributed to CC-induced neutrophil necrosis,
362 which was pyroptosis rather than necroptosis or NETosis. Moreover, GSDMD played a
363 role in the activation of β_2 integrin and the maturation process of neutrophils, both of
364 which promote neutrophil migration into inflamed tissues. Both prophylactic and
365 therapeutic administration of DSF protected CC-injected mice from crystal clot formation,
366 AKI, and kidney infarction. These findings identify GSDMD as a key mediator of focal
367 crystalline TMA and its consequences ischemic tissue infarction and organ failure.
368 Several previous studies have implicated the involvement of GSDMD and pyroptosis
369 in driving AKI, but these findings have yielded conflicting results.[26-28] However, various
370 conditions of a model disease context may account for this virtual discrepancy. In CC-
371 induced TMA, we observed an upregulation of activated caspase-1 and GSDMD protein
372 expression in immune cells in the kidneys, and the NLRP3 inhibitor MCC950 has
373 exhibited a protective effect against ischemic necroinflammation.[3] Furthermore, CCs
374 themselves have been identified as inducers of the NLRP3 inflammasome.[12,13] Hence,
375 focal crystalline TMA involves robust inflammasome activation, a major upstream event
376 in GSDMD activation and subsequent pathogenesis. Importantly, previous studies[26,27]

Downloaded from http://ashpublications.net/blood/article-pdf/doi/10.1182/blood.2023021949/2223568/blood.2023021949.pdf by guest on 06 May 2024

have predominantly focused on tubular epithelial cells, where GSDMD and pyroptosis are activated downstream of caspase-4, 5, and 11. In contrast, our findings indicate predominant expression of GSDMD in peritubular interstitial cells in the TMA kidney, and the absence of *Gsdmd* in tubular epithelial cells did not affect the levels of hypoxia-induced necrosis. Moreover, it has been reported that protein expression of GSDMD is undetectable in lysates of specifically isolated mouse kidney tubules.[28] Based on our observations, we speculate that infiltrating leukocytes, particularly neutrophils that massively evolve only hours after the embolic event, serve as cellular origin of GSDMD in the development of TMA.

It has been reported that CC induces neutrophil necrosis as a form of necroptosis[29] and NETosis.[14] In our investigation, GSDMD regulates CC-induced neutrophil pyroptosis and the release of IL-1β. Importantly, this observation indicates an active and specific process facilitated by GSDMD, rather than being a passive event associated with necroptosis. IL-1β is a highly potent proinflammatory mediator that stimulates the recruitment of neutrophils to the site of inflammation.[30,31] Moreover, platelets further boost the inflammasome and subsequent release of IL-1β from neutrophils.[32] Hence, neutrophil-derived IL-1β in response to CC serves to amplify the pathogenesis of focal crystalline TMA, exacerbating both immunothrombosis and necroinflammation. In contrast, our findings suggest that CC-induced NET formation occurs independently of GSDMD while both histone and CC-activated platelets trigger NET formation in a GSDMD dependent manner. Consequently, the observed reduction in kidney tissue and intravascular NETs detected in *Gsdmd*$^{-/-}$ mice with focal crystalline TMA could arise from decreased levels of histone released by necrotic tubular cells, reduced neutrophil infiltration and limited NET formation. Previous studies have reported that caspase-11 or neutrophil elastase can

Downloaded from http://ashpublications.net/blood/article-pdf/doi/10.1182/blood.2023021949/2223568/blood.2023021949.pdf by guest on 06 May 2024

activate GSDMD, thereby promoting NET formation,[8,9] and GSDMD pores can elevate cytoplasmic calcium concentrations and activate protein arginine deiminase-4 (PAD4), leading to histone citrullination.[9] However, since CC induces NETs in a PAD4-independent manner,[14] it is possible that GSDMD does not influence this process. Similarly, neutrophils lacking GSDMD remained capable of forming NETs when stimulated with phorbol 12-myristate 13-acetate or calcium ionophore.[18,33] Therefore, the role of GSDMD in NETosis is stimulus-dependent and requires further investigation.

We observed a decrease in the population of circulating and kidney-infiltrating mature neutrophils in response to focal TMA in *Gsdmd*$^{-/-}$ mice, while the number of neutrophils in bone marrow and spleen, sites for emergency granulopoiesis during inflammatory conditions,[34,35] and lung, where neutrophils emigrate from inflammation sites before redirecting to bone marrow for withdrawal,[36] remained unchanged. This suggests that the reduced neutrophil numbers in blood and kidney of *Gsdmd*$^{-/-}$ mice with focal TMA did not arise from an alteration in neutrophil development nor homing. Indeed, under homeostatic condition GSDMD-deficiency had no impact on neutrophil numbers and their maturation in vivo, as well as during iPSC-derived neutrophil differentiation. Nevertheless, *Gsdmd*-deficiency reduced the number of mature neutrophils in bone marrow, spleen, and blood after focal TMA. The expression of CXCR2 was diminished in *Gsdmd*$^{-/-}$ bone marrow neutrophils in response to the maturation factor G-CSF or TNFα after 24 hours in vitro stimulation, indicating an active involvement of GSDMD in neutrophil maturation under inflammatory condition. This impaired neutrophil maturation could ultimately lead to a reduced CXCR2 and β_2 integrin-mediated[22] migration of mature neutrophils into the blood and kidney in *Gsdmd*$^{-/-}$ mice after focal TMA. However, several questions remain unanswered: when do neutrophils acquire

Downloaded from http://ashpublications.net/blood/article-pdf/doi/10.1182/blood.2023021949/2223568/blood.2023021949.pdf by guest on 06 May 2024

GSDMD proteins? How does GSDMD regulate β_2 integrin activation? Does GSDMD also modulate ageing or reverse migration processes? Given the complex and heterogenous nature of neutrophil maturation,[37,38] further investigation is needed to elucidate the precise role of GSDMD during this process.

Considering the role of GSDMD as the final downstream effector in the inflammasome and pyroptosis/IL-1β pathways, targeting GSDMD presents a potentially effective and precise strategy. DSF, originally used in the management of chronic alcohol addiction by acting upon aldehyde dehydrogenase, has also been recognized as an inhibitor of GSDMD through a high-throughput biochemical screening. It covalently modifies Cys191 and blocks GSDMD pore formation, thereby preventing pyroptosis and the release of IL-1β.[39] Notably, DSF protected mice against sepsis induced by LPS[39] as well as cecal ligation and puncture.[10] Our study demonstrated the prophylactic and therapeutic effects of DSF on CC-induced TMA and its consequences, suggesting a potential therapeutic approach including the administration of the drug prior to catheterization, a major trigger for CC embolism as a form of focal crystalline TMA. Given that CC-induced TMA and various forms of TMA share a common pathogenesis initially induced by immunothrombosis, inhibiting GSDMD holds a potential for ameliorating TMA in a broader context.

Our study has a series of limitations. Although we focused on investigating the role of GSDMD in neutrophils, *Gsdmd*$^{-/-}$ mice do not fully exclude the possibility of GSDMD also contributing to the overall phenotype in other cell types. Using cell type-specific tools will be necessary to address these aspects in detail. Moreover, DSF, used as a tool to study GSDMD effects in both in vitro and in vivo settings, may not possess absolute selectivity as an inhibitor, thus allowing for potential off-target effects. Of note, the animal

Downloaded from http://ashpublications.net/blood/article-pdf/doi/10.1182/blood.2023021949/2223568/blood.2023021949.pdf by guest on 06 May 2024

449 model used in this study represents a focal TMA within the kidney, which may not fully
450 replicate all hematological features of systemic TMA such as hemolytic anemia.

451 Together, GSDMD contributes to the development of crystalline TMA of the kidney
452 and its consequences, ischemic kidney infarction and kidney failure (Supplementary
453 figure S16). As GSDMD actively contributes to neutrophil maturation and the induction
454 of inflammatory pyroptosis in neutrophils, which prominently evolve within only a few
455 hours following an embolic event, prophylactic as well as therapeutic GSDMD blockade
456 can effectively prevent focal TMA and its associated consequences. The same process
457 should apply to other organs in the body affected by the same disease, and may apply to
458 systemic forms of TMA, which share a common pathogenesis that initially triggers
459 immunothrombosis with subsequent ischemic necroinflammation and organ failure.

Downloaded from http://ashpublications.net/blood/article-pdf/doi/10.1182/blood.2023021949/2223568/blood.2023021949.pdf by guest on 06 May 2024

Declarations

Acknowledgment

We thank Yvonne Minor and Uschi Kögelsperger for animal husbandry, and Janina Mandelbaum and Anna Anfimiadou for expert technical support. Experiments were performed using a Nikon Eclipse Ti2 microscope system (funded by DFG GZ:INST 86/1851-1 FUGG to Prof. Martha Merrow).

Authors' Contributions

H-J.A and S.S.: Funding and supervision. K.W-K., S.S., and H-J.A.: Conceptualization. K.W-K. and S.S.: Methodology. K.W-K.: Investigation. K.W-K., C.L., K.J., L.H., H.C., and M.K.: Data analysis. K.W-K., E.M-B., K.V.A., M.R., and O.S.: Visualization. M.I.L. and C.K.: Differentiation of iPSC-derived neutrophils with gene editing. K.W-K., H.C., B.A., and E.M-B.: Flow chamber experiments. T.S.B.H., D.Z., and Y.K.: Protocol and suggestions. A.L.: Resources. K.W-K. and H-J.A.: Writing original drafts. All authors read and revised the manuscript.

Funding

This project was supported by the Deutsche Forschungsgemeinschaft (TRR332, projects A2, A7, B1, Z1, and AN372/20-2 and 30-1). K.W-K. was supported by Takeda Science Foundation.

Conflict of interest

The authors declare no competing financial interests.

Downloaded from http://ashpublications.net/blood/article-pdf/doi/10.1182/blood.2023021949/2223568/blood.2023021949.pdf by guest on 06 May 2024

References

1. George JN, Nester CM. Syndromes of thrombotic microangiopathy. *N Engl J Med*. 2014;371(7):654-666.

2. Jokiranta TS. HUS and atypical HUS. *Blood*. 2017;129(21):2847-2856.

3. Shi C, Kim T, Steiger S, et al. Crystal Clots as Therapeutic Target in Cholesterol Crystal Embolism. *Circ Res*. 2020.

4. Genest DS, Patriquin CJ, Licht C, John R, Reich HN. Renal Thrombotic Microangiopathy: A Review. *Am J Kidney Dis*. 2023;81(5):591-605.

5. Shi J, Zhao Y, Wang K, et al. Cleavage of GSDMD by inflammatory caspases determines pyroptotic cell death. *Nature*. 2015;526(7575):660-665.

6. Liu X, Xia S, Zhang Z, Wu H, Lieberman J. Channelling inflammation: gasdermins in physiology and disease. *Nat Rev Drug Discov*. 2021;20(5):384-405.

7. Kayagaki N, Stowe IB, Lee BL, et al. Caspase-11 cleaves gasdermin D for non-canonical inflammasome signalling. *Nature*. 2015;526(7575):666-671.

8. Sollberger G, Choidas A, Burn GL, et al. Gasdermin D plays a vital role in the generation of neutrophil extracellular traps. *Sci Immunol*. 2018;3(26).

9. Chen KW, Monteleone M, Boucher D, et al. Noncanonical inflammasome signaling elicits gasdermin D-dependent neutrophil extracellular traps. *Sci Immunol*. 2018;3(26).

10. Silva CM, Wanderley CWS, Veras FP, et al. Gasdermin D inhibition prevents multiple organ dysfunction during sepsis by blocking NET formation. *Blood*. 2021.

11. Mulay SR, Linkermann A, Anders HJ. Necroinflammation in Kidney Disease. *J Am Soc Nephrol*. 2016;27(1):27-39.

12. Duewell P, Kono H, Rayner KJ, et al. NLRP3 inflammasomes are required for

Downloaded from http://ashpublications.net/blood/article-pdf/doi/10.1182/blood.2023021949/2223568/blood.2023021949.pdf by guest on 06 May 2024

507 atherogenesis and activated by cholesterol crystals. *Nature*. 2010;464(7293):1357-1361.
508 13. Tall AR, Yvan-Charvet L. Cholesterol, inflammation and innate immunity. *Nat*
509 *Rev Immunol*. 2015;15(2):104-116.
510 14. Warnatsch A, Ioannou M, Wang Q, Papayannopoulos V. Inflammation.
511 Neutrophil extracellular traps license macrophages for cytokine production in
512 atherosclerosis. *Science*. 2015;349(6245):316-320.
513 15. Engelmann B, Massberg S. Thrombosis as an intravascular effector of innate
514 immunity. *Nat Rev Immunol*. 2013;13(1):34-45.
515 16. Kilkenny C, Browne WJ, Cuthill IC, Emerson M, Altman DG. Improving
516 bioscience research reporting: the ARRIVE guidelines for reporting animal research.
517 *PLoS Biol*. 2010;8(6):e1000412.
518 17. Nakazawa D, Kumar SV, Marschner J, et al. Histones and Neutrophil
519 Extracellular Traps Enhance Tubular Necrosis and Remote Organ Injury in Ischemic AKI.
520 *J Am Soc Nephrol*. 2017;28(6):1753-1768.
521 18. Chauhan D, Demon D, Vande Walle L, et al. GSDMD drives canonical
522 inflammasome-induced neutrophil pyroptosis and is dispensable for NETosis. *EMBO Rep*.
523 2022:e54277.
524 19. Yao W, Chen Y, Li Z, et al. Single Cell RNA Sequencing Identifies a Unique
525 Inflammatory Macrophage Subset as a Druggable Target for Alleviating Acute Kidney
526 Injury. *Adv Sci (Weinh)*. 2022;9(12):e2103675.
527 20. Xie X, Shi Q, Wu P, et al. Single-cell transcriptome profiling reveals neutrophil
528 heterogeneity in homeostasis and infection. *Nat Immunol*. 2020;21(9):1119-1133.
529 21. Kolaczkowska E, Kubes P. Neutrophil recruitment and function in health and
530 inflammation. *Nat Rev Immunol*. 2013;13(3):159-175.

Downloaded from http://ashpublications.net/blood/article-pdf/doi/10.1182/blood.2023021949/2223568/blood.2023021949.pdf by guest on 06 May 2024

22. Silvestre-Roig C, Hidalgo A, Soehnlein O. Neutrophil heterogeneity: implications for homeostasis and pathogenesis. *Blood*. 2016;127(18):2173-2181.

23. Ma Q, Immler R, Pruenster M, et al. Soluble uric acid inhibits β2 integrin-mediated neutrophil recruitment in innate immunity. *Blood*. 2022;139(23):3402-3417.

24. Nemeth T, Sperandio M, Mocsai A. Neutrophils as emerging therapeutic targets. *Nat Rev Drug Discov*. 2020;19(4):253-275.

25. Schaefer SL, Hummer G. Sublytic gasdermin-D pores captured in atomistic molecular simulations. *Elife*. 2022;11.

26. Miao N, Yin F, Xie H, et al. The cleavage of gasdermin D by caspase-11 promotes tubular epithelial cell pyroptosis and urinary IL-18 excretion in acute kidney injury. *Kidney Int*. 2019;96(5):1105-1120.

27. Zhang Z, Shao X, Jiang N, et al. Caspase-11-mediated tubular epithelial pyroptosis underlies contrast-induced acute kidney injury. *Cell Death Dis*. 2018;9(10):983.

28. Tonnus W, Maremonti F, Belavgeni A, et al. Gasdermin D-deficient mice are hypersensitive to acute kidney injury. *Cell Death Dis*. 2022;13(9):792.

29. Desai J, Foresto-Neto O, Honarpisheh M, et al. Particles of different sizes and shapes induce neutrophil necroptosis followed by the release of neutrophil extracellular trap-like chromatin. *Sci Rep*. 2017;7(1):15003.

30. Schett G, Dayer JM, Manger B. Interleukin-1 function and role in rheumatic disease. *Nat Rev Rheumatol*. 2016;12(1):14-24.

31. Miller LS, O'Connell RM, Gutierrez MA, et al. MyD88 mediates neutrophil recruitment initiated by IL-1R but not TLR2 activation in immunity against Staphylococcus aureus. *Immunity*. 2006;24(1):79-91.

Downloaded from http://ashpublications.net/blood/article-pdf/doi/10.1182/blood.2023021949/2223568/blood.2023021949.pdf by guest on 06 May 2024

555 32. Rolfes V, Ribeiro LS, Hawwari I, et al. Platelets Fuel the Inflammasome
556 Activation of Innate Immune Cells. *Cell Rep*. 2020;31(6):107615.
557 33. Wang X, Blanco LP, Carmona-Rivera C, et al. Effects of Gasdermin D in
558 Modulating Murine Lupus and its Associated Organ Damage. *Arthritis Rheumatol*.
559 2020;72(12):2118-2129.
560 34. Manz MG, Boettcher S. Emergency granulopoiesis. *Nat Rev Immunol*.
561 2014;14(5):302-314.
562 35. Inra CN, Zhou BO, Acar M, et al. A perisinusoidal niche for extramedullary
563 haematopoiesis in the spleen. *Nature*. 2015;527(7579):466-471.
564 36. Silvestre-Roig C, Braster Q, Ortega-Gomez A, Soehnlein O. Neutrophils as
565 regulators of cardiovascular inflammation. *Nat Rev Cardiol*. 2020;17(6):327-340.
566 37. Ng LG, Ostuni R, Hidalgo A. Heterogeneity of neutrophils. *Nat Rev Immunol*.
567 2019;19(4):255-265.
568 38. Palomino-Segura M, Sicilia J, Ballesteros I, Hidalgo A. Strategies of neutrophil
569 diversification. *Nat Immunol*. 2023.
570 39. Hu JJ, Liu X, Xia S, et al. FDA-approved disulfiram inhibits pyroptosis by
571 blocking gasdermin D pore formation. *Nat Immunol*. 2020;21(7):736-745.
572

Downloaded from http://ashpublications.net/blood/article-pdf/doi/10.1182/blood.2023021949/2223568/blood.2023021949.pdf by guest on 06 May 2024

Figure legends

Figure 1. GSDMD is expressed in neutrophils during their maturation and is activated upon focal crystalline TMA

A) Illustration of the study design presented in the published dataset. Cells were sorted from the kidney, blood, and spleen of C57BL/6J mice before (D0), and on day 1 (D1) and day 3 (D3) after unilateral ischemia-reperfusion injury (uIRI).

B) Uniform Manifold Approximation and Projection (UMAP) plot of a total of 80829 cells following quality control. Clusters 3 and 15 were identified as neutrophils based on representative neutrophil gene expression.

C) UMAP plot of 7467 neutrophils, categorized into eight clusters (G0-4 and G5a-c), representing different maturation stages. Clusters G0, G1, G2, G3 and G4 corresponded to granulocyte monocyte progenitor, pro-neutrophil, pre-neutrophil, immature neutrophil, and mature neutrophil in bone marrow. The names, pro-neutrophil, pre-neutrophil, immature neutrophil, and mature neutrophil were adopted from the previous report.[37] Clusters G5a-c represent the most mature neutrophils present in peripheral blood.

D) Dot plot representing the expression profile of gasdermin D (Gsdmd) for each cluster. The dot color indicates the average gene expression level in each cluster, while the dot size represents the percentage of cells in each cluster.

E) UMAP plot of Gsdmd expression in neutrophils across different organs.

F) Representative MACSima images of cholesterol crystal (CC)-induced thrombotic microangiopathy (TMA) and contralateral sham kidneys from wild-type (WT) mice. High magnification views 1, 2, and 4 of TMA kidney represents intravascular thrombotic occlusion with platelets and neutrophil extracellular traps, while high

Downloaded from http://ashpublications.net/blood/article-pdf/doi/10.1182/blood.2023021949/2223568/blood.2023021949.pdf by guest on 06 May 2024

magnification view 3 represents neutrophil accumulation in periinfarct region. Gray: 4',6-diamidino-2-phenylindole (DAPI), red: Ly6G, yellow: citrullinated histone 3 (CitH3), purple: smooth muscle actin (SMA), blue: cleaved caspase-3, cyan: Ly6C (in the sham kidney and low magnification of TMA kidney) or CD41 (in high magnification views 1-4 of TMA kidney).

G) Representative immunofluorescent images of thrombotic occlusion of the kidney artery. TER-119-positive erythrocytes (red) and CD41-positive platelets (green) within αSMA-positive arteries (cyan) in TMA and sham kidneys from WT mice. Nuclei were visualized with DAPI (blue).

H) Representative immunohistochemical images of GSDMD staining on TMA and sham kidneys of WT and *Gsdmd*$^{-/-}$ mice.

I) Immunoblot analysis of GSDMD (pro and cleaved p30 (N-terminal fragment)) and caspase-1 (pro and cleaved p20) in the WT kidneys of two sets of healthy control (HC) and focal TMA mice. β-actin was used as a loading control.

J) Immunoblot analysis of GSDMD in immune cells isolated from TMA and healthy kidneys from WT mice. Immune cells from four kidneys per group were pooled and analyzed. β-actin was used as a loading control.

K) Flow cytometric quantification of caspase1 activation within neutrophils (CD45+ CD11b+ Ly6G+) in TMA and sham kidneys from WT mice.

L) Representative histogram for caspase1 activation within neutrophils in the kidneys.

Scale bars: (F) 1000 μm in the sham kidney and low magnification of TMA kidney, or 50 μm in high magnification views 1-4 of TMA kidney. (G) and (H) 20 μm. The data represent means ± SD. ***$p < 0.001$ using unpaired Student's t-test.

Downloaded from http://ashpublications.net/blood/article-pdf/doi/10.1182/blood.2023021949/2223568/blood.2023021949.pdf by guest on 06 May 2024

Figure 2. *Gsdmd* deficiency attenuates focal crystalline TMA, acute kidney injury, and ischemic infarction

A) Illustration of the experimental design. Cholesterol crystal (CC) (20 mg/kg) was injected into the left renal artery to induce focal thrombotic microangiopathy (TMA) in wild-type (WT) and gasdermin D knockout (*Gsdmd*$^{-/-}$) mice. The mice were sacrificed and analyzed after 24 hours.

B) Representative immunohistochemical images of alpha-smooth muscle actin (αSMA) and fibrin staining of interlobar, arcuate, and interlobular arteries in kidneys.

C) Quantification of arterial obstruction of sham (n=13) and TMA kidneys from WT (n=10) and *Gsdmd*$^{-/-}$ (n=13) mice.

D) Representative immunohistochemical images of αSMA and fibrin staining within glomerular capillaries.

E) Representative images of Periodic acid-Schiff (PAS) staining within glomeruli, showing characteristics indicative of TMA, including glomerular capillary thrombi and increased capillary wall thickness.

F) Quantification of glomerular fibrin thrombi in sham (n=4) and TMA kidneys from WT (n=6) and *Gsdmd*$^{-/-}$ (n=6) mice.

G) Glomerular filtration rate (GFR) at baseline and 24 hours after focal TMA induction in WT mice (n=16) and *Gsdmd*$^{-/-}$ mice (n=18).

H) Representative images of 2,3,5-Triphenyltetrazolium chloride (TTC) staining on the TMA (left) and sham (contralateral right) kidneys of WT and *Gsdmd*$^{-/-}$ mice. The red areas indicate living kidney tissue, while the white areas indicate infarcted kidney tissue.

I) Quantification of the infarct size of sham (n=25) and TMA kidneys from WT (n=12)

Downloaded from http://ashpublications.net/blood/article-pdf/doi/10.1182/blood.2023021949/2223568/blood.2023021949.pdf by guest on 06 May 2024

and *Gsdmd*$^{-/-}$ (n=13) mice.

J) Representative images of PAS staining on sham and TMA kidneys of WT and *Gsdmd*$^{-/-}$ mice.

K) Quantification of tubular injury of sham (n=13) and TMA kidneys from WT (n=10) and *Gsdmd*$^{-/-}$ (n=13) mice.

L) Immunoblot analysis of mature IL-1β (p17) in the kidneys of three sets of sham, WT and *Gsdmd*$^{-/-}$ mice with focal TMA. β-actin was used as a loading control.

M) Plasma levels of IL-1β in healthy mice (n=6) and focal TMA mice (WT: n=9, *Gsdmd*$^{-/-}$: n=9) quantified by ELISA.

Scale bars: (B), (D), (E), and (J) 20 μm, (H) 4 mm. The data represent means ± SD. *$p < 0.05$, **$p < 0.01$, and ***$p < 0.001$ using two-way ANOVA with Bonferroni's multiple comparisons test (C, G), or one-way ANOVA with Tukey's post-hoc test (F, I, K, M).

Figure 3. Neutrophil recruitment and maturation are impaired in *Gsdmd*$^{-/-}$ mice with focal TMA

A) Representative gating of flow cytometric analysis for the quantification of neutrophils (CD45+ CD11b+ Ly6G+) and monocytes (CD45+ CD11b+ Ly6C+) in blood and kidney from wild-type (WT) and gasdermin D knockout (*Gsdmd*$^{-/-}$) mice with focal thrombotic microangiopathy (TMA) (24 hours).

B)-C) Percentage of neutrophils among CD45+ cells (B) and their absolute number (C) in blood from healthy mice (n=6) and focal TMA mice (WT: n=8, *Gsdmd*$^{-/-}$: n=8).

D)-E) Percentage of neutrophils among CD45+ cells (D) and their absolute number (E) in sham (n=4) and TMA kidneys from WT (n=12) and *Gsdmd*$^{-/-}$ (n=11) mice.

F) Representative gating of flow cytometric analysis for the quantification of mature

Downloaded from http://ashpublications.net/blood/article-pdf/doi/10.1182/blood.2023021949/2223568/blood.2023021949.pdf by guest on 06 May 2024

(CD45+ CD11b+ Ly6G+ CD101+) and immature (CD45+ CD11b+ Ly6G+ CD101-) neutrophils in bone marrow, spleen, and blood from WT and *Gsdmd*$^{-/-}$ mice with focal TMA.

G)-I) Percentage of mature neutrophils among CD45+ CD11b+ Ly6G+ neutrophils in bone marrow (G), spleen (H), and blood (I) from healthy mice (n=9) and focal TMA mice (WT: n=4, *Gsdmd*$^{-/-}$: n=3).

J)-L) Percentage of mature and immature neutrophils among CD45+ cells in bone marrow (J), spleen (K), and blood (L) from healthy mice (n=9) and focal TMA mice (WT: n=4, *Gsdmd*$^{-/-}$: n=3).

M) Bone marrow cells isolated from WT and *Gsdmd*$^{-/-}$ healthy mice were incubated for 24 hours with or without granulocyte colony-stimulating factor (G-CSF, 100 ng/mL) or tumor necrosis factor alpha (TNFα, 20 ng/mL). The expression levels of CXCR2 in mature neutrophils (Ly6G+ CD101+) were quantified as mean fluorescence intensity (MFI) using flow cytometry. Data are representative of three independent experiments.

N) The expression levels of β_2 integrin macrophage-1 antigen (MAC-1) in bone marrow neutrophils from healthy mice (n=5) and focal TMA mice (WT: n=8, *Gsdmd*$^{-/-}$: n=7), shown as MFI quantified by flow cytometry.

The data represent means ± SD. *$p < 0.05$, **$p < 0.01$, and ***$p < 0.001$ using one-way ANOVA with Tukey's post-hoc test (B-E, G-I, N) or two-way ANOVA with Bonferroni's multiple comparisons test (J-M).

Figure 4. *Gsdmd* deficiency reduces NETs in both kidney arteries and tissue necroinflammation in focal TMA

A) Representative immunofluorescent images of neutrophil extracellular traps (NETs),

Downloaded from http://ashpublications.net/blood/article-pdf/doi/10.1182/blood.2023021949/2223568/blood.2023021949.pdf by guest on 06 May 2024

identified as citrullinated histone 3 (CitH3)-positive area (green) originating from Ly6G-positive neutrophils (cyan), within alpha-smooth muscle actin (αSMA)-positive arteries (red) in the thrombotic microangiopathy (TMA) kidney. DNA was visualized with 4',6-diamidino-2-phenylindole (DAPI, blue).

B) Representative immunofluorescent images of Ly6G-positive neutrophils (red) and CD41-positive platelets (cyan) within αSMA-positive arteries (green) in TMA kidneys. DNA was visualized with DAPI (blue).

C)-F) Quantification of CitH3 (C), Ly6G (D), CD41 (E), as well as Ly6G and CD41 (F)-positive area within αSMA-positive arteries in TMA kidneys from wild-type (WT) and gasdermin D knockout (*Gsdmd*$^{-/-}$) mice (n=3-4 per group).

G) Representative immunofluorescent images of NETs in the periinfarct of TMA kidneys, identified as CitH3-positive area (green) originating from Ly6G-positive neutrophils (red). DNA was visualized with DAPI (blue).

H) Quantification of CitH3-positive area in the periinfarct of sham (n=4) and TMA kidneys from WT (n=8) and *Gsdmd*$^{-/-}$ (n=8) mice.

I) Absolute number of NETing neutrophils (CD45+ CD11b+ Ly6G+ CitH3+) in sham (n=4) and TMA kidneys from WT (n=8) and *Gsdmd*$^{-/-}$ (n=8) mice, determined by flow cytometry.

Scale bars: (A) and (B) 20 μm, (G) 50 μm (low magnification) and 20 μm (high magnification). The data represent means ± SD. *$p < 0.05$ using unpaired Student's t-test (C-F), or one-way ANOVA with Tukey's post-hoc test (H, I).

Figure 5. Disulfiram inhibits CC-induced neutrophil pyroptosis in human neutrophils

Downloaded from http://ashpublications.net/blood/article-pdf/doi/10.1182/blood.2023021949/2223568/blood.2023021949.pdf by guest on 06 May 2024

A) Human neutrophils were primed with lipopolysaccharide (LPS) for 2 hours, then stimulated with cholesterol crystal (CC) or nigericin (10 μM) for 3 hours under shaking conditions. Cell-free supernatants were collected for interleukin (IL)-1β ELISA.

B) Human neutrophils were primed with LPS for 2 hours, then stimulated with or without CC (1 mg/mL) for 3 hours under shaking conditions. Cell-free supernatants and cell lysates from 3 wells were combined for each condition and collected for immunoblot analysis of gasdermin D (GSDMD) and IL-1β. β-actin was used as a loading control.

C)-D) Human neutrophils were primed with LPS for 2 hours. After pretreatment with disulfiram (DSF), VX-765, necrostatin-1s (Nec-1s), and necrosulfonamide (NSA), the cells were stimulated with CC (1 mg/mL) for 3 hours under shaking conditions. Cell-free supernatants were collected for IL-1β ELISA (C) and lactate dehydrogenase (LDH) assay (D).

E) Representative immunofluorescent and live images of neutrophil extracellular traps (NETs). Human neutrophils were incubated on CC-precoated slides for 4 hours, with or without DSF or dimethyl sulfoxide (DMSO) treatment. NETs were visualized by immunofluorescent images, stained with citrullinated histone 3 (CitH3, green), myeloperoxidase (MPO, red), and 4',6-diamidino-2-phenylindole (DAPI, blue), and by live cell images stained with SYTOX Green (SG, green).

F) Human neutrophils were primed with CXCL8. After pretreatment with DSF, diphenyleneiodonium chloride (DPI), or DMSO, the cells were stimulated with CC (0.6 mg/mL) for 3 hours under shaking conditions. The cells were stained with SG for flow cytometric analysis.

G) Representative histogram for SG positive neutrophils.

Downloaded from http://ashpublications.net/blood/article-pdf/doi/10.1182/blood.2023021949/2223568/blood.2023021949.pdf by guest on 06 May 2024

H) Heparinized whole blood samples from wild-type (WT) mice were perfused over the collagen-coated surface at 1000 s^{-1} in the presence and absence of CC using a flow chamber system. In a second-step flow chamber assay, RedDeep Tracker-fluorescently labelled WT and *Gsdmd*$^{-/-}$ bone marrow neutrophils were perfused over platelet-rich thrombi through the chamber at 500 s^{-1}.

I) Platelets and neutrophils were stained by anti-CD41 (green), RedDeep (cyan), and CitH3 (red) antibodies and visualized using immunofluorescence confocal microscopy. Nuclei were stained with DAPI (blue).

J)-K) Quantification of the ratio between CD41 (platelet marker) and RedDeep-neutrophils (J) and CitH3 signals (K) (n=4 per group).

Scale bars: (E) 20 μm (immunofluorescent images) and 100 μm (live images), (I) 10 μm. The data represent means ± SEM (A, C, D, F) or SD (J, K). *p < 0.05, **p < 0.01, and ***p < 0.001 using one-way ANOVA with Dunnett's multiple comparisons test (A, C, D, F), or two-way ANOVA with Bonferroni's multiple comparisons test (J, K). Data are representative of at least two independent experiments.

Figure 6. *GSDMD*-deficient iPSC-derived human neutrophils resist CC-induced pyroptosis and β_2 integrin activation

A) Immunoblot analysis of gasdermin D (GSDMD) in induced pluripotent stem cell (iPSC)-derived neutrophils, performed on control and two distinct *GSDMD*-knockout clones. β-actin was used as a loading control.

B) Immunoblot analysis of GSDMD in control iPSC-derived neutrophils cultured at day 18 (undifferentiated time point) and day 38 (differentiated time point).

C)-D) iPSC-derived neutrophils were primed with lipopolysaccharide (LPS) for 4 hours,

Downloaded from http://ashpublications.net/blood/article-pdf/doi/10.1182/blood.2023021949/2223568/blood.2023021949.pdf by guest on 06 May 2024

765 followed by stimulation with cholesterol crystal (CC, 1.5 mg/mL) for 3 hours under
766 shaking conditions. Cell-free supernatants were collected for interleukin (IL)-1β ELISA
767 (C) and lactate dehydrogenase (LDH) assay (D).
768 E)-F) iPSC-derived neutrophils were stimulated with or without CXCL8 (100 ng/mL) for
769 10 minutes. Surface expression levels of β_2 integrins LFA-1 (E) and MAC-1 (F) were
770 quantified as a mean fluorescence intensity (MFI) using flow cytometry.
771 G) Representative immunofluorescent and live images of neutrophil extracellular traps
772 (NETs). iPSC-derived neutrophils were incubated on CC-precoated slides for 4 hours.
773 NETs were visualized by immunofluorescent images, stained with citrullinated
774 histone 3 (CitH3, green), myeloperoxidase (MPO, red), and 4',6-diamidino-2-
775 phenylindole (DAPI, blue), and by live cell images stained with SYTOX Green (SG,
776 green).
777 H) iPSC-derived neutrophils were primed with CXCL8, then stimulated with CC (1.0
778 mg/mL) for 3 hours under shaking conditions. The cells were stained with SG for
779 flow cytometric analysis.
780 I) Representative histogram for SG positive iPSC-derived neutrophils.
781 Scale bars: (G) 10 μm (immunofluorescent images) and 100 μm (live images). The data
782 represent means ± SEM. ***$p < 0.001$ using two-way ANOVA with Dunnett's multiple
783 comparisons test. Data are representative of four to five independent experiments.
784
785 **Figure 7. Therapeutic disulfiram protects mice from TMA, AKI and ischemic**
786 **infarction**
787 A) Illustration of the experimental design. Wild-type (WT) mice were administered
788 disulfiram (DSF, 50 mg/kg) or vehicle 3 hours following cholesterol crystal (CC)

Downloaded from http://ashpublications.net/blood/article-pdf/doi/10.1182/blood.2023021949/2223568/blood.2023021949.pdf by guest on 06 May 2024

induced thrombotic microangiopathy (TMA) in the kidney. The mice were sacrificed and analyzed 24 hours post-surgery.

B) Representative immunohistochemical images of alpha-smooth muscle actin (αSMA) and fibrin staining of interlobar, arcuate, and interlobular arteries in TMA kidneys.

C) Quantification of arterial obstruction (n=3-4 per group).

D) Glomerular filtration rate (GFR) at baseline and 24 hours after focal TMA induction (n=4 per group).

E) Representative images of 2,3,5-Triphenyltetrazolium chloride (TTC) staining on the TMA (left) and sham (contralateral right) kidneys. The red areas indicate living kidney tissue, while the white areas indicate infarcted kidney tissue.

F) Quantification of the kidney infarct size (n=4 per group).

G) Representative images of Periodic acid-Schiff (PAS) staining on TMA kidneys.

H) Quantification of tubular injury (n=4 per group).

I) Representative gating of flow cytometric analysis for the quantification of neutrophils (CD45+ CD11b+ Ly6G+) and monocytes (CD45+ CD11b+ Ly6C+) in blood and kidney following focal TMA induction.

J)-K) Percentage of neutrophils among CD45+ cells (J) and their absolute number (K) in blood from healthy mice (n=10) and focal TMA mice (n=4 per group).

L)-M) Percentage of neutrophils among CD45+ cells (L) and their absolute number (M) in TMA kidneys (n=3-4 per group).

N) Absolute number of NETing neutrophils (CD45+ CD11b+ Ly6G+ CitH3+) in TMA kidneys (n=4 per group) determined by flow cytometry.

Scale bars: (B) and (G) 20 μm, (E) 4 mm. The data represent means ± SD. *$p < 0.05$, **$p < 0.01$, and ***$p < 0.001$ using two-way ANOVA with Bonferroni's multiple comparisons

Downloaded from http://ashpublications.net/blood/article-pdf/doi/10.1182/blood.2023021949/2223568/blood.2023021949.pdf by guest on 06 May 2024

813 test (C), or one-way ANOVA with Tukey's post-hoc test (D, F, H, J-N).

814

Downloaded from http://ashpublications.net/blood/article-pdf/doi/10.1182/blood.2023021949/2223568/blood.2023021949.pdf by guest on 06 May 2024

Figure 1

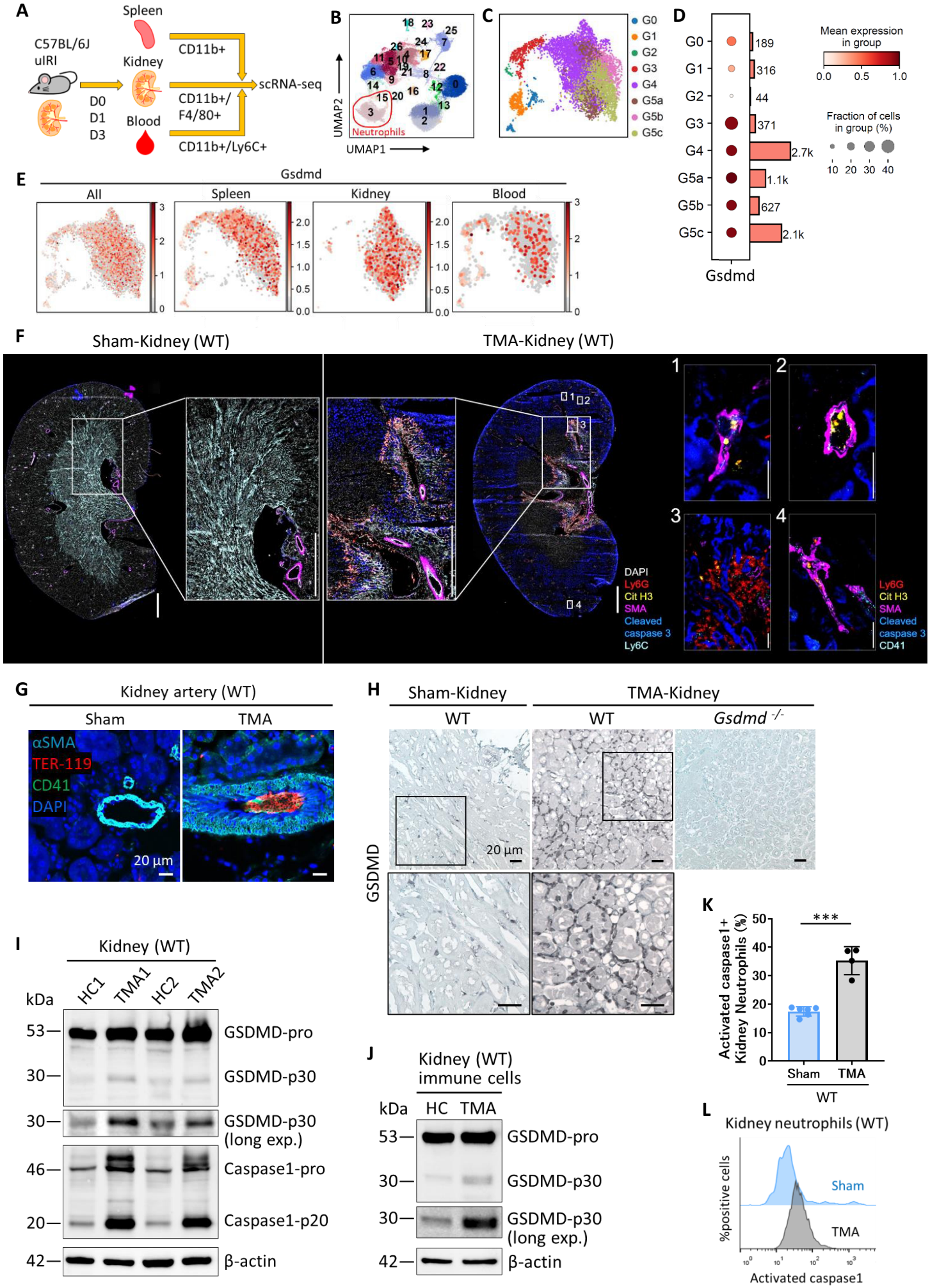

Downloaded from http://ashpublications.net/blood/article-pdf/doi/10.1182/blood.2023021949/2223568/blood.2023021949.pdf by guest on 06 May 2024

Figure 2

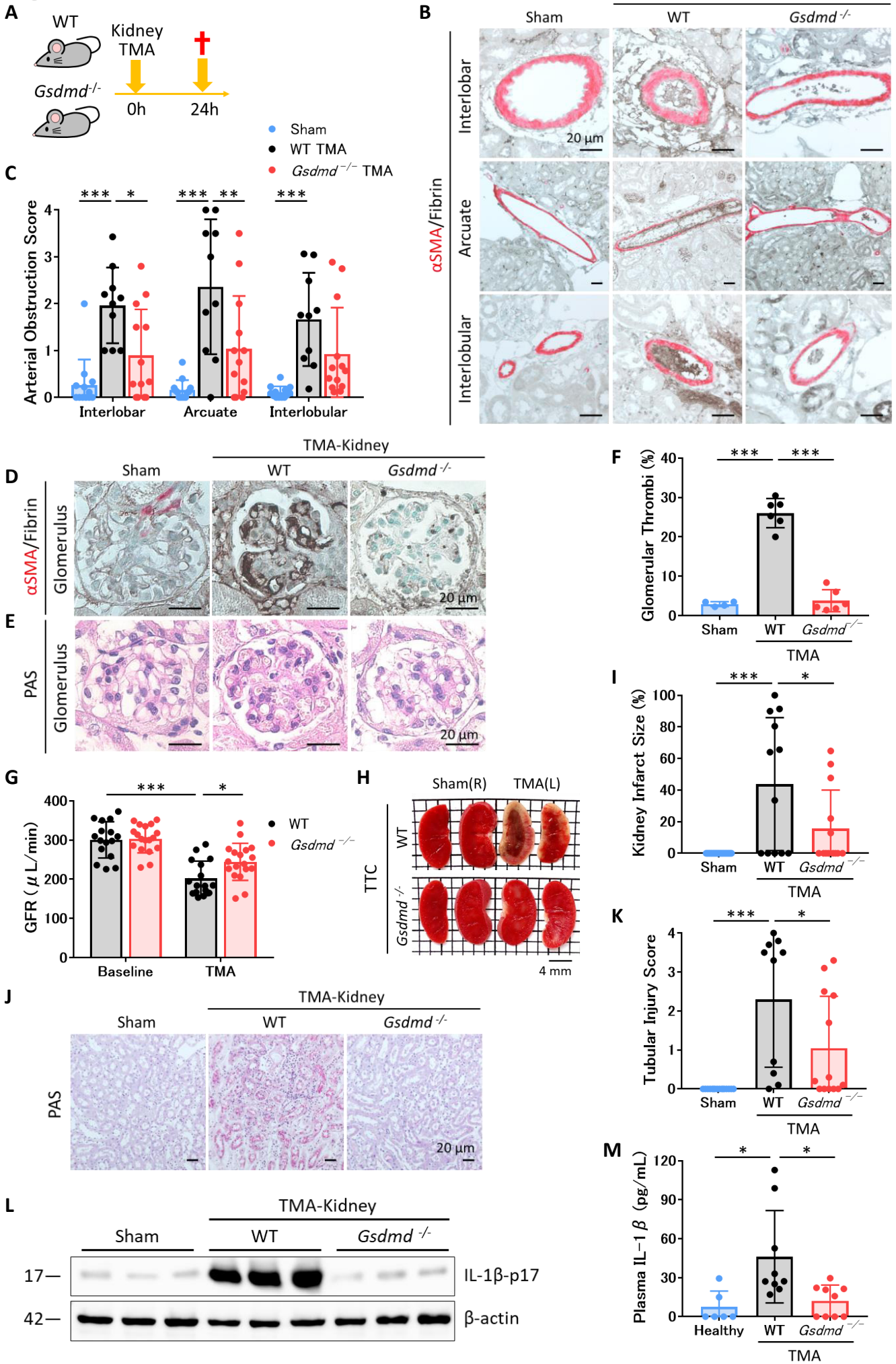

Downloaded from http://ashpublications.net/blood/article-pdf/doi/10.1182/blood.2023021949/2223568/blood.2023021949.pdf by guest on 06 May 2024

Figure 3

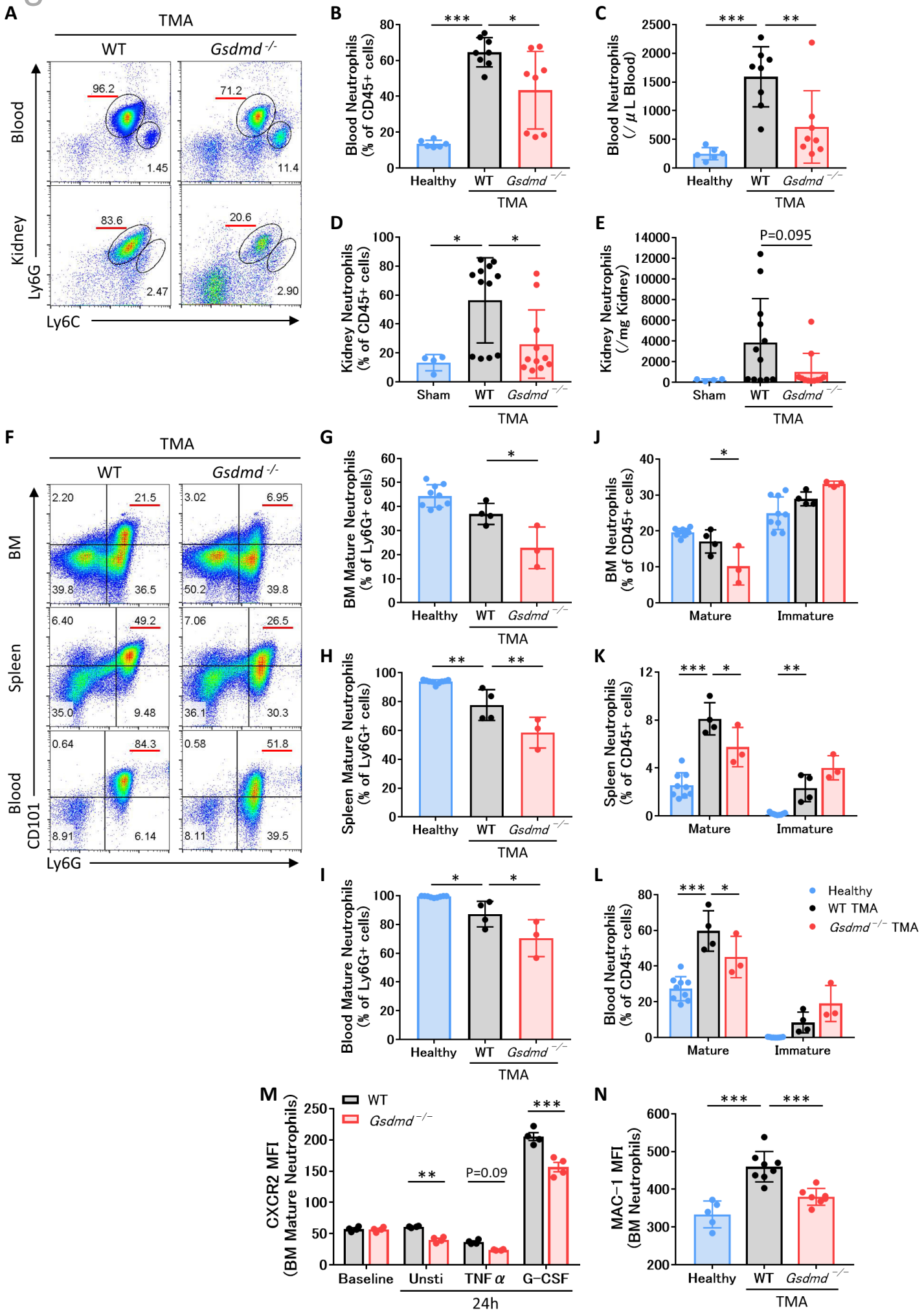

Downloaded from http://ashpublications.net/blood/article-pdf/doi/10.1182/blood.2023021949/2223568/blood.2023021949.pdf by guest on 06 May 2024

Figure 4

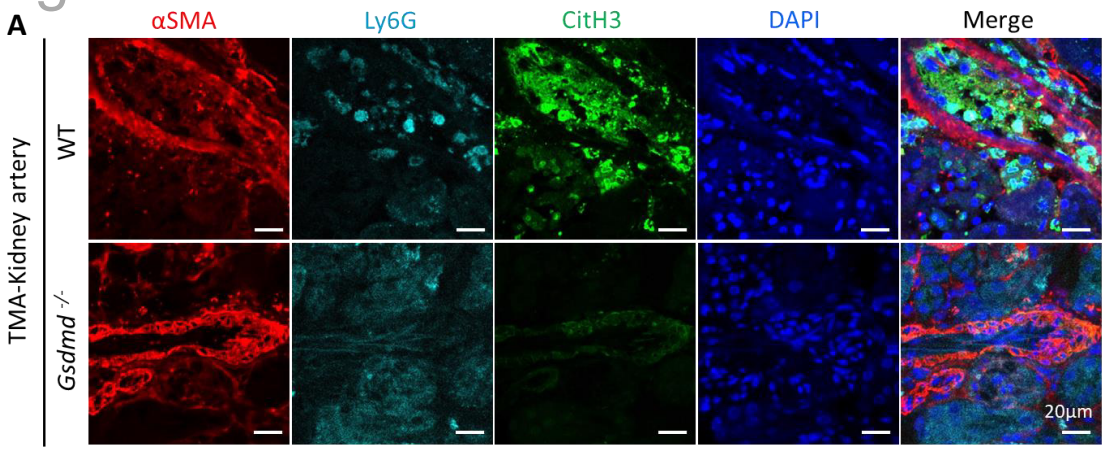

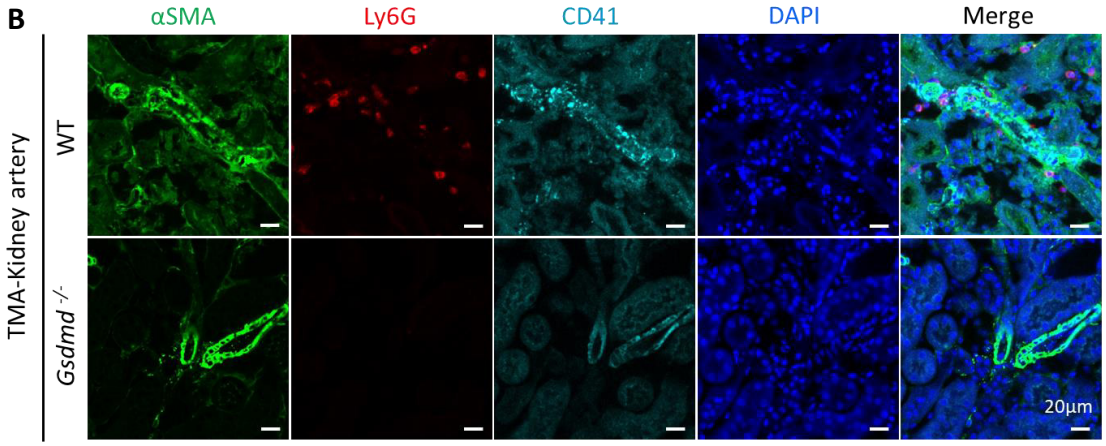

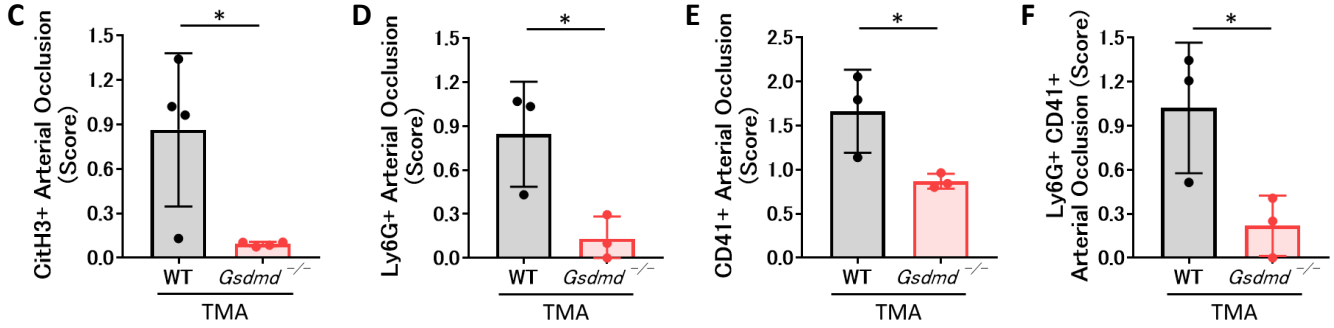

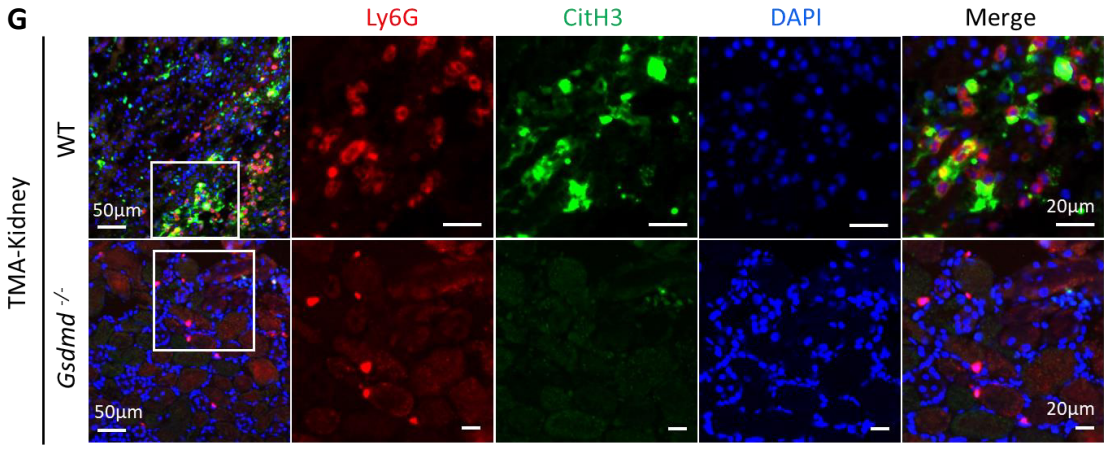

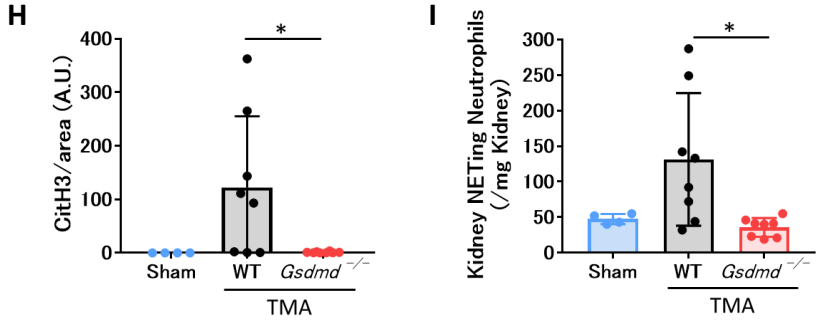

Downloaded from http://ashpublications.net/blood/article-pdf/doi/10.1182/blood.2023021949/2223568/blood.2023021949.pdf by guest on 06 May 2024

Figure 5

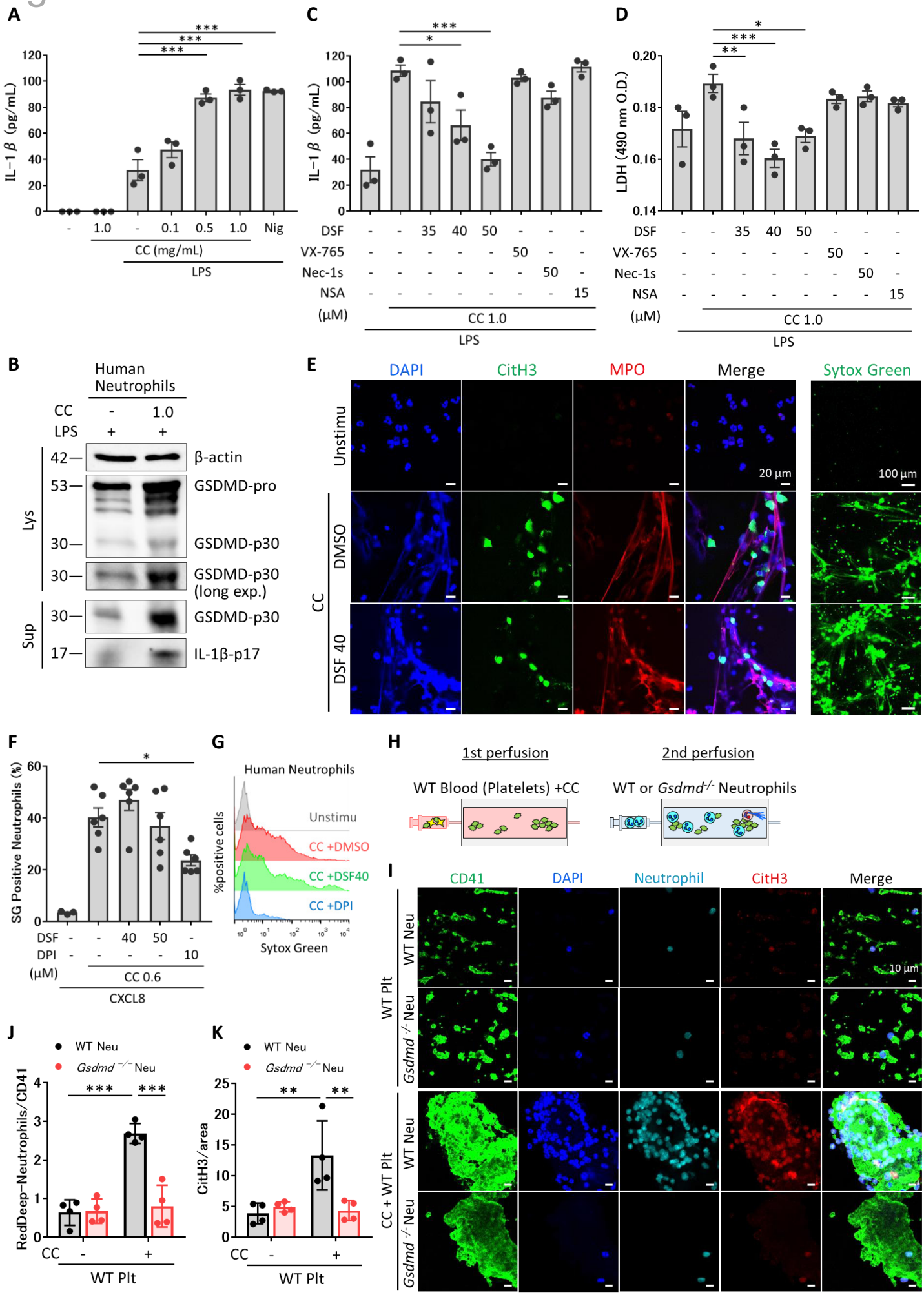

Downloaded from http://ashpublications.net/blood/article-pdf/doi/10.1182/blood.2023021949/2223568/blood.2023021949.pdf by guest on 06 May 2024

Figure 6

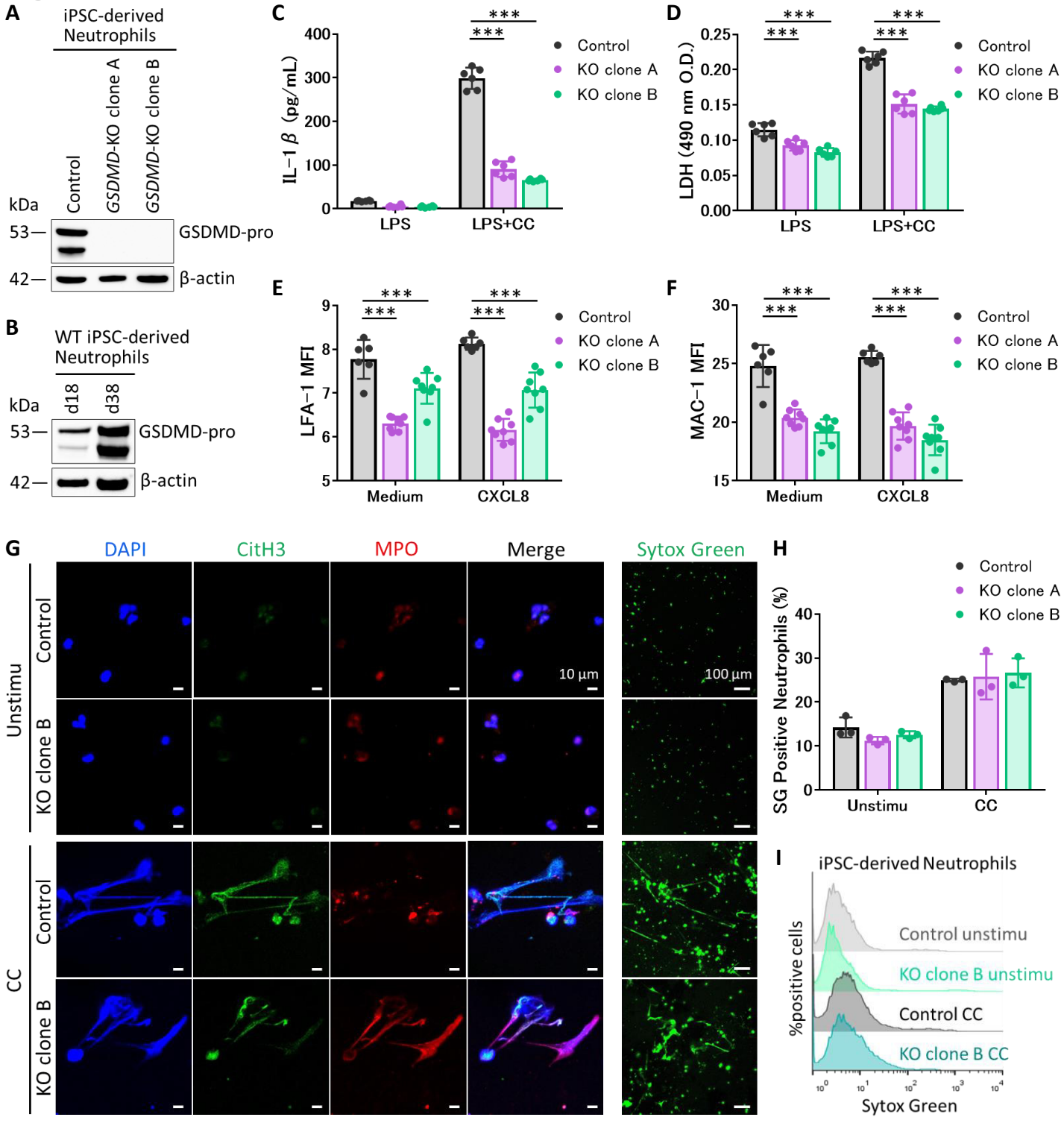

Downloaded from http://ashpublications.net/blood/article-pdf/doi/10.1182/blood.2023021949/2223568/blood.2023021949.pdf by guest on 06 May 2024

Figure 7

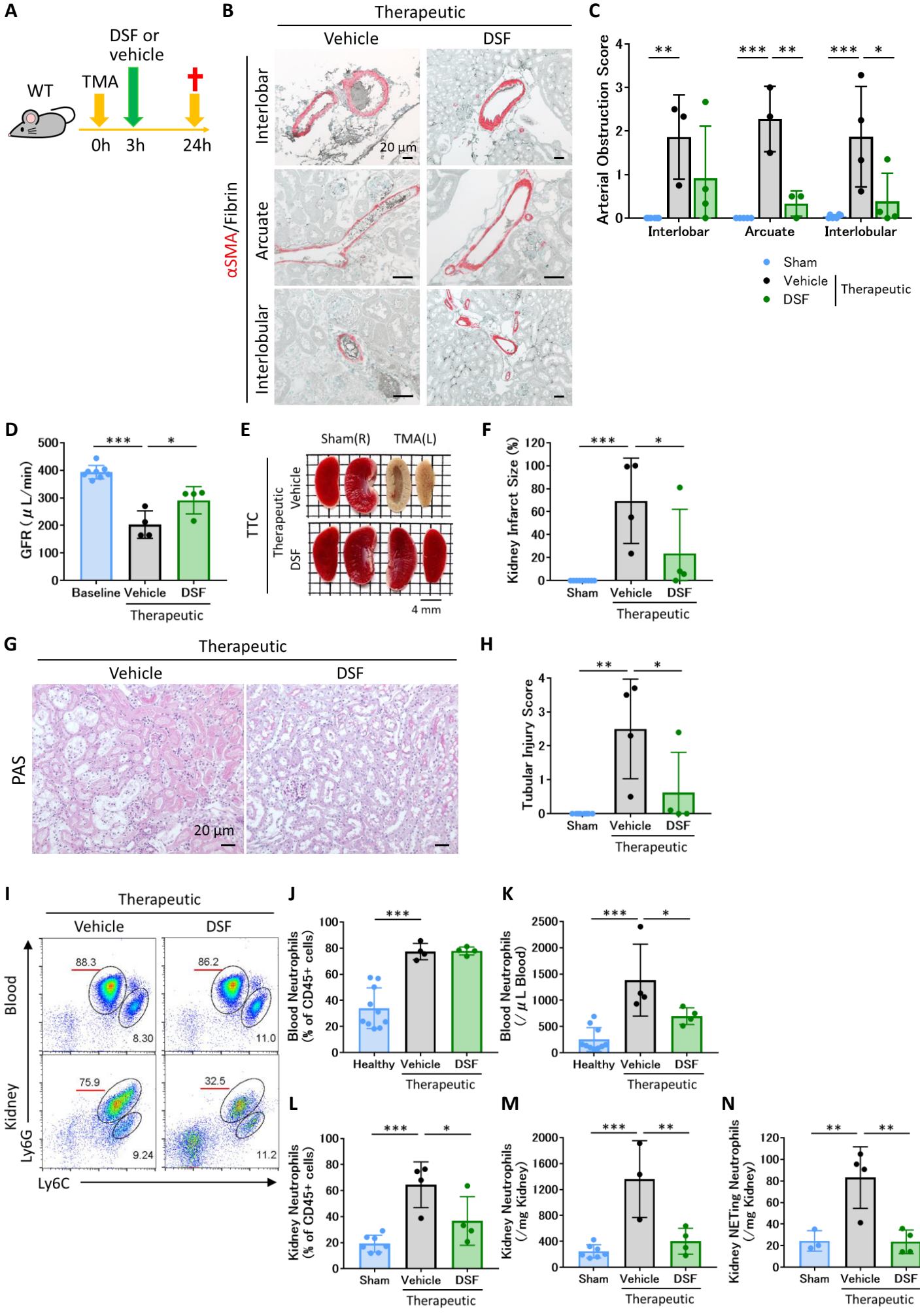

Downloaded from http://ashpublications.net/blood/article-pdf/doi/10.1182/blood.2023021949/2223568/blood.2023021949.pdf by guest on 06 May 2024

Role of Gasdermin D in Cholesterol Crystal-Induced Focal Thrombotic Microangiopathy (TMA)

Context or Research: Thrombotic microangiopathy is characterized by microvascular immunothrombosis and ischemic tissue injury, leading to organ failure

Working hypothesis: Gasdermin D (GSDMD) contributes to TMA and its consequences by amplifying neutrophil maturation and subsequent necrosis

Findings

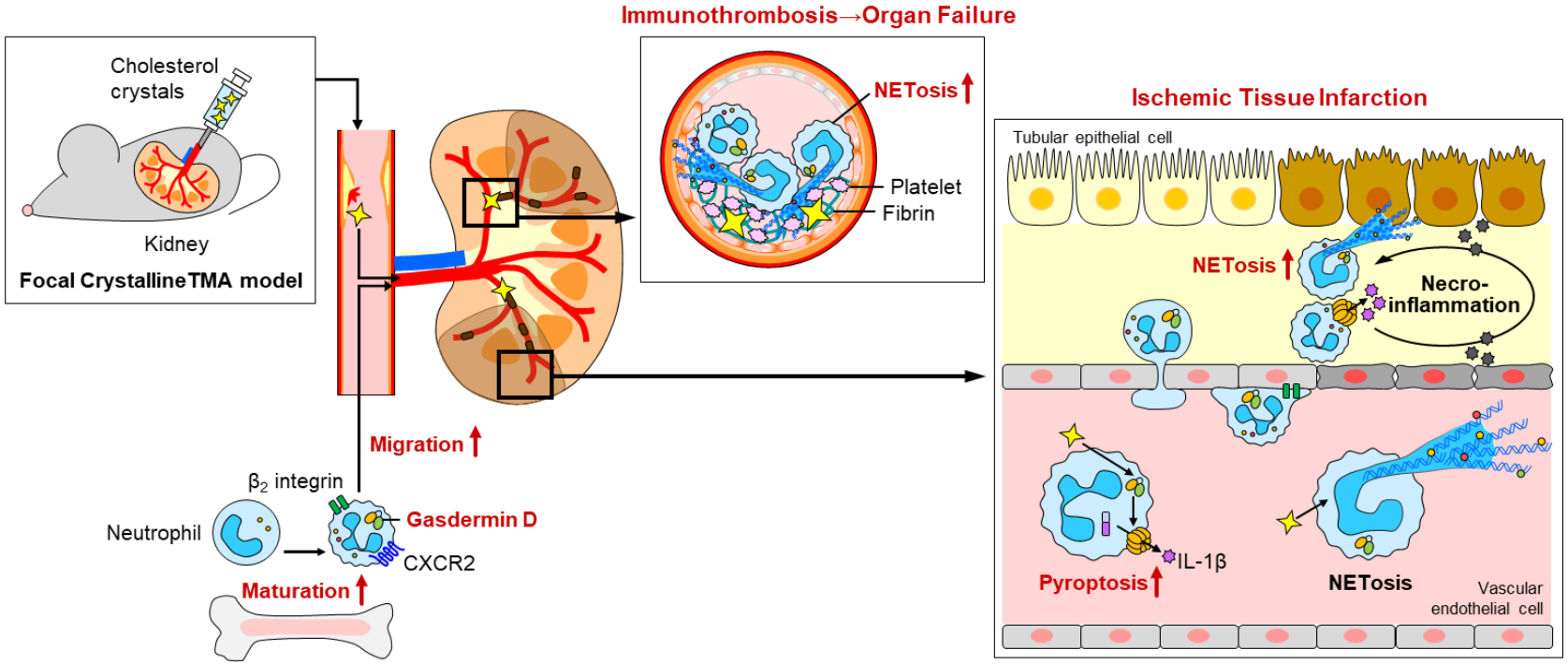

Conclusions: 1) Gasdermin D contributes to focal crystalline TMA and its consequences: ischemic tissue infarction and organ failure. 2) Gasdermin D drives neutrophil necrosis, maturation, and tissue recruitment during focal crystalline TMA.

*Watanabe-Kusunoki et al. DOI: 10.xxxx/**blood**.2024xxxxxx*

Blood Visual Abstract

Downloaded from http://ashpublications.net/blood/article-pdf/doi/10.1182/blood.2023021949/2223568/blood.2023021949.pdf by guest on 06 May 2024